


Cite this: *RSC Adv.*, 2025, 15, 14315

# Progress on liposome delivery systems in the treatment of bladder cancer

Xinyu Guo,<sup>†ab</sup> Yan Zhang,<sup>†c</sup> Quanyong Liu,<sup>ab</sup> Mingquan Xu,<sup>ab</sup> Jianzhi Pang,<sup>b</sup> Bin Yang,<sup>d</sup> Shuo Rong<sup>\*e</sup> and Xiaofeng Yang<sup>\*ab</sup>

Bladder cancer (BC) in the urinary system remains one of the most prevalent malignancies with high recurrence rate globally. Current treatment schemes against BC such as surgery, chemotherapy, and radiotherapy have substantial limitations including side effects, drug resistance, and poor tumor targeting. Considering the above-mentioned challenges, nanotechnology has become a current research hotspot, particularly liposome-based drug delivery systems, which offer promising novel therapeutic strategies aimed at reducing systemic toxicity, overcoming drug resistance, and enhancing drug targeting. This review systematically elaborates the current research progress on liposomal drug delivery systems in BC treatment, focusing on their application in chemotherapy, immunotherapy, and gene therapy. Additionally, we provide a comprehensive assessment of the benefits and limitations of liposome nanocarriers used in BC treatment. The advanced targeting strategies and combination treatments via liposomal therapies are also discussed, demonstrating that liposomal formulations have great potential application value in the treatment of BC owing to their superior bioavailability, stability, and targeting and minimal adverse effects.

Received 3rd February 2025

Accepted 8th April 2025

DOI: 10.1039/d5ra00746a

rsc.li/rsc-advances

## 1. Introduction

Bladder cancer (BC) is the second most common urological malignancy worldwide and is characterized by significant intra-tumoral heterogeneity.<sup>1</sup> The prognosis of BC largely depends on the presence or absence of muscle invasion. Approximately 75% of bladder tumors are non-muscle invasive (NMIBC) at diagnosis. The primary treatment for NMIBC is transurethral resection of the bladder tumor (TURBT), followed by intravesical chemotherapy infusion or immunotherapy to prevent disease recurrence and progression. Common intravesical chemotherapeutic agents include gemcitabine and mitomycin, which have been proven to be effective in preventing the implantation of residual tumor cells and reducing the recurrence risk. Epirubicin and mitomycin are also frequently used, and Bacillus Calmette–Guérin (BCG) is another common

intravesical agent for NMIBC.<sup>2–4</sup> However, despite these therapies, around 40% of NMIBC cases recur, and 10% progress to more advanced stages.<sup>5</sup>

Muscle-invasive bladder cancer (MIBC) needs more aggressive management than NMIBC, often requiring neoadjuvant chemotherapy, radical cystectomy, and pelvic lymph node dissection. However, nearly 30% of patients experience poor prognoses owing to its high risk of metastasis.<sup>6</sup> For MIBC and advanced BC, platinum-based combination chemotherapy, which includes regimens such as methotrexate, vinblastine, doxorubicin (DOX), and cisplatin (MVAC) or gemcitabine–cisplatin/carboplatin (GC), is the standard treatment. In cases where patients are ineligible for cystectomy, adjuvant or palliative radiotherapy can be applied to realize local tumor control and increase the survival rate.<sup>7,8</sup>

Although surgery, chemotherapy, and radiotherapy have significantly contributed to BC treatment, their efficacy remains limited by several factors. Tumor cell metastasis reduces the effectiveness of surgery, and chemotherapy and radiotherapy are associated with considerable side effects to vital organs. Moreover, the occurrence and development of drug resistance further reduce their effectiveness, leading to a significant challenge in BC treatment.<sup>9–11</sup> In recent years, immunotherapy and targeted therapy have advanced rapidly. Compared with traditional chemotherapy, PD-1/L1 monoclonal antibody-based immunotherapy has markedly improved the overall survival rate in patients with advanced BC.<sup>12–14</sup> Additionally, immune checkpoint inhibitors such as CTLA-4 and CAR T-cell therapy

<sup>a</sup>Department of Urology Surgery, First Hospital of Shanxi Medical University, Taiyuan, Shanxi, 030001, China. E-mail: yxfylq@163.com

<sup>b</sup>The First Clinical Medical College of Shanxi Medical University, Taiyuan, Shanxi, 030001, China

<sup>c</sup>School of Optoelectronic Engineering, Xi'an Technological University, Xi'an, 710021, China

<sup>d</sup>Department of Urology, Shanxi Bethune Hospital, Shanxi Academy of Medical Sciences, Third Hospital of Shanxi Medical University, Tongji Shanxi Hospital, Taiyuan, 030032, China

<sup>e</sup>Third Hospital of Shanxi Medical University, Shanxi Bethune Hospital, Shanxi Academy of Medical Sciences, Tongji Shanxi Hospital, Taiyuan, 030032, China. E-mail: qs20060606@163.com

<sup>†</sup> These authors contributed equally.


have been introduced in BC treatment. However, despite these advancements, immune evasion mechanisms in BC cells continue to limit the efficacy of immunotherapy.<sup>15</sup>

Nanotechnology, with its targeted delivery capabilities, biocompatibility, and enhanced bioavailability compared to conventional drugs, has already been applied for drug delivery in many fields.<sup>16–18</sup> In BC treatment, nano-sized drug delivery systems, especially liposomes have been extensively employed. These systems can be modified with polyethylene glycol (PEG) to evade the reticuloendothelial system (RES), thereby improving the drug delivery efficiency and enhancing *in vivo* stability.<sup>19,20</sup> They are capable of encapsulating amphiphilic drugs, achieving the simultaneous delivery of multiple therapeutic agents. Additionally, liposomal systems can effectively enhance the effect of chemotherapy owing to their ease of surface functionalization, targeted delivery capabilities, and ability to stabilize drugs *in vivo* (Fig. 1).

Recently, LPs have been utilized for delivering cargo (drugs and genes), which can be alone or in combination with various targeting strategies in BC treatment. The functionalization of the surface of liposomes with antibody fragments<sup>21</sup> has also been employed to achieve the targeted delivery of multiple chemotherapeutic<sup>22</sup> or immunotherapeutic agents.<sup>23</sup> Here, temperature,<sup>24,25</sup> pH,<sup>26</sup> magnetic field,<sup>21</sup> ultrasound,<sup>27</sup> and photodynamic signals<sup>28</sup> as physicochemical and biological stimuli have been applied for controlled targeting. Notably, these strategies applied to cancer drugs have presented promising results (Fig. 2).<sup>29–31</sup>

In this review, we introduce the common methods for the synthesis of liposomes, their key characterization parameters and typical functionalization strategies. Then, we provide an overview of current research on liposome-based therapies for BC, including chemotherapeutic and nucleic acid delivery, immunotherapy, photodynamic therapy (PDT) and stimuli-responsive liposomes (temperature, pH, US, *etc.*). Besides, their characteristic of easy modification and efficient combination with other techniques can further enhance the efficacy and safety of tumor treatment. Also, the key challenges and obstacles in drug delivery and the clinical translation of BC treatment are discussed.

## 2. Methods for the preparation of liposomes

Liposome synthesis technology is an important research direction in the field of drug delivery, where the process for the

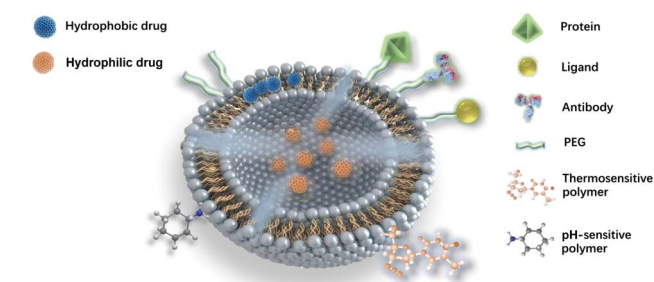


Fig. 1 Schematic of different types of functionalized liposomes.

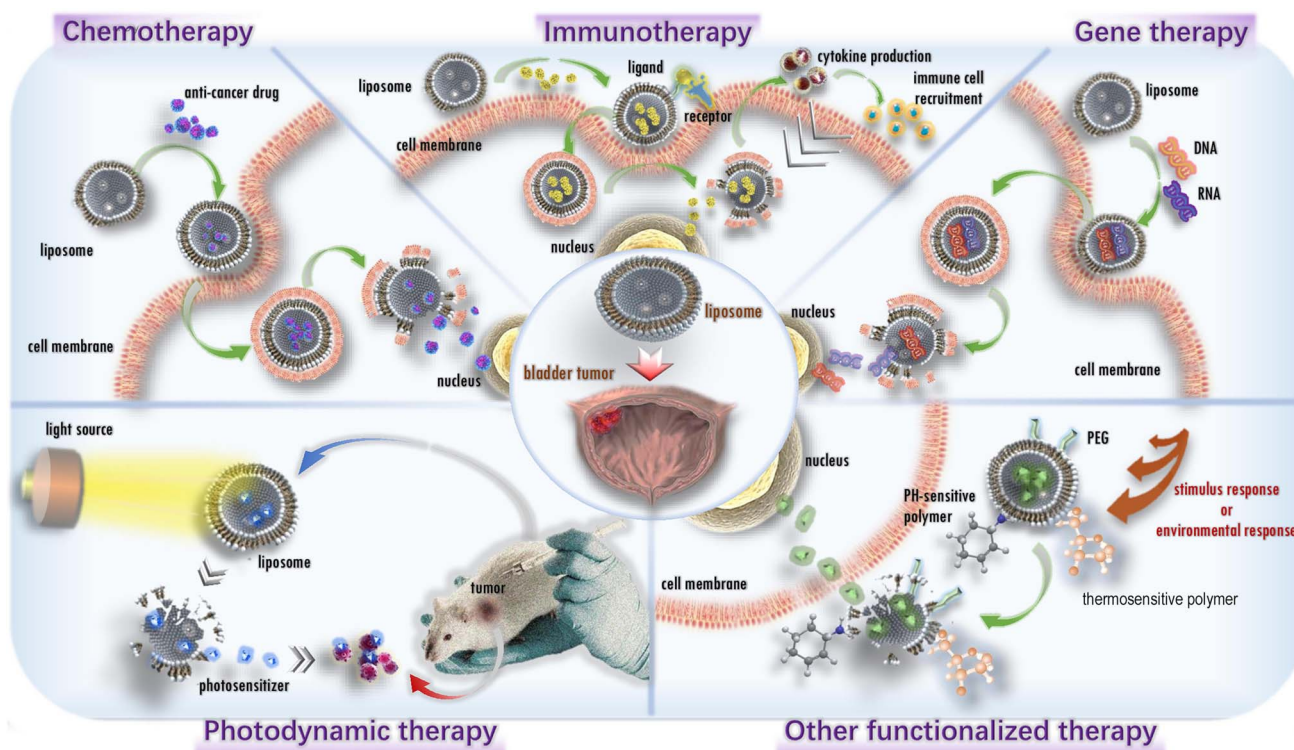


Fig. 2 Schematic of liposome-based drug delivery systems in BC treatment.



**Table 1** Names of liposome synthesis techniques, their suitable carrier types, along with their advantages, disadvantages, and an overview of the synthesis process

Synthesis method	Drug type	Advantages	Disadvantages	Description
Thin film hydration	Lipophilic	Simple, suitable for large-scale production	Heterogeneous liposome sizes, low encapsulation efficiency	Dissolved in an organic solvent → evaporated to form thin film → hydrated
Reverse phase evaporation	Hydrophilic/amphiphilic	High encapsulation efficiency	Residual organic solvents, complex preparation process	Oil-in-water (O/W) emulsion is formed → sonication or agitation → removal organic solvent
Solvent injection	Lipophilic	Rapid process with high controllability	Heterogeneous liposome size, requiring post-processing	Dissolved in an organic solvent → rapidly injected into an aqueous phase → liposome formation
Detergent removal	Lipophilic/amphiphilic	Suitable for preparing unilamellar liposomes with uniform size	Time-consuming, detergent residues	Mixed micelles formed using detergents → dialysis or chromatography → liposome self-assembly
Freeze-thaw method	Hydrophilic/amphiphilic	Suitable for encapsulating macromolecules, high encapsulation efficiency	Liposome aggregation, affecting stability	Liposomal suspensions → repeated freeze-thaw cycles → forming large unilamellar vesicles
pH gradient	Hydrophilic	Fast process without organic solvents	Limited applicability, requiring precise pH adjustment	Rapid increase in pH → formation of small unilamellar vesicles
Ammonium sulfate gradient	Hydrophilic	Suitable for hydrophilic drugs with high encapsulation efficiency	Requires additional gradient formation steps, complex	Preparation ammonium sulfate solution → removal of external ammonium sulfate → drug loading
Microfluidics	Hydrophilic/lipophilic	Precise size control, suitable for industrial production	Requires complex equipment and high costs	A microfluidic device precisely controls the mixing of lipid and aqueous phases → uniformly sized liposomes

preparation of liposomes involves a variety of methods and techniques, including liposome formulation and size modulation. Different synthesis techniques significantly influence the final properties of liposomes, such as particle size, lamellar structure, and encapsulation efficiency.<sup>32</sup> Each of these methods has unique characteristics and suitable for specific research needs and production scales. Herein, we focus on the most commonly used liposome synthesis techniques at the laboratory scale. Table 1 presents the names of the liposome synthesis techniques, their suitable carrier types, their advantages, disadvantages, and an overview of the synthesis process.

### 2.1 Thin film hydration

The thin-film hydration method is the classic and straightforward method for the preparation of liposomes, which is widely applied in the development of drug delivery systems. Initially, lipids are dissolved in organic solvents (*e.g.*, chloroform or methanol), followed by vacuum drying to form a uniform film on the container walls. Subsequently, a buffer solution is added to the container, thus inducing the redispersion of the lipid film through a hydration process to form liposomes. The hydration parameters play a critical role in determining the structures of vesicle, where mild stirring typically produces large unilamellar vesicles (GUVs), while intense agitation yields multilamellar vesicles (MLVs). For further optimization of the size and uniformity of liposome, techniques such as sonication and polycarbonate membrane extrusion can be employed.<sup>33</sup>

This method is particularly effective for encapsulating lipophilic compounds, achieving encapsulation efficiencies of over 90%. In contrast, the encapsulation efficiency for hydrophilic substances generally ranges between 10% and 30%.<sup>34</sup> Its advantages include simplicity, cost-effectiveness, and versatility in drug loading, establishing its significance in liposome research.

### 2.2 Reverse phase evaporation

The reverse-phase evaporation method is an efficient technique for liposome preparation, which is particularly suitable for encapsulating hydrophilic drugs. In this method, phospholipids are first dissolved in an organic solvent (*e.g.*, chloroform) that is immiscible with water, while the drug is dissolved in the aqueous phase. A water-in-oil (w/o) emulsion is formed through sonication, followed by the slow evaporation of the organic solvent under reduced pressure to produce a gel phase. Further removal of the solvent results in the aqueous phase being highly encapsulated within the liposome core, forming a liposome dispersion.<sup>35</sup>

One of the key advantages of this method is its high encapsulation efficiency, with the passive encapsulation efficiency for hydrophilic drugs reaching 30–50%. This efficiency can be increased to over 90% when combined with active loading techniques.<sup>36</sup> Additionally, the reverse-phase evaporation method is well-suited for the preparation of small-volume injectable formulations.<sup>34</sup>

### 2.3 Microfluidics

Microfluidics is an emerging technique for the preparation of liposomes, enabling efficient and homogeneous production by precisely controlling the mixing and reaction of nanoliter-scale fluids. The core innovation of microfluidics is the “solvent displacement method,” where nanoprecipitation is initiated by mixing polar solvents (*e.g.*, alcohols and water) to drive lipid self-assembly into spherical liposomes.<sup>37,38</sup>

One of the key advantages of microfluidics is its ability to achieve high homogeneity by adjusting the solvent ratios and flow rates, allowing precise control of the liposome size and distribution, while minimizing the inter-batch variability.<sup>39</sup> Additionally, this method simplifies the process steps by integrating lipid hydration and extrusion into a single-step operation, significantly improving the production efficiency. Microfluidics also enables the encapsulation of both hydrophilic and hydrophobic drugs, making it suitable for a wide range of active ingredients, including small molecules,<sup>40,41</sup> nucleic acids,<sup>42</sup> and proteins.<sup>43</sup>

## 3. Methods for the characterization of liposomes

The characterization of liposomes is essential for understanding their physicochemical properties, optimizing formulation design, and ensuring their efficacy as drug delivery systems. Key parameters, including size, polydispersity index (PDI), zeta potential, morphology, encapsulation efficiency (EE), and drug release, play a critical role in assessing the performance of liposomes.

These key characterization parameters serve as standardized metrics for evaluating the quality and performance of liposome formulations, enabling the objective optimization of the lipid composition, ratios, and synthesis conditions. In the following sections, we discuss these characterization techniques in detail. Table 2 provides a summary of the key characterization parameters, analytical techniques, and assay standards for liposomal formulations.

### 3.1 Size and PDI

The size and polydispersity index (PDI) of liposomes are key parameters that determine their drug encapsulation efficiency, *in vivo* circulation time, and stability.<sup>44,45</sup> Their size and PDI are commonly measured using DLS, which calculates these parameters based on changes in the scattered light intensity and NTA, which provides more accurate results by tracking the motion of individual particles. Smaller-sized liposomes (typically  $\leq 100$  nm) are more likely to evade uptake by the immune system and prolong their circulatory half-life, whereas larger-sized liposomes are cleared more quickly.<sup>46,47</sup> Therefore, liposomes used for drug delivery typically have a size in the range of 50–200 nm.<sup>48,49</sup> The size of liposomes can be precisely controlled through techniques such as extrusion, sonication, homogenization, and microfluidics.

PDI is a measure of the uniformity of the size distribution of liposomes, ranging from 0 to 1. A PDI of  $\leq 0.3$  indicates a uniform size distribution, making the liposomes suitable for drug delivery applications. In contrast, a PDI of  $>0.3$  suggests a broad size distribution or the presence of multiple liposome populations, which may lead to instability and inconsistent drug release.<sup>50</sup>

### 3.2 Zeta potential

The surface charge of a liposome is primarily determined by its lipid head group, which can be classified as positive, negative, or amphipathic, and is influenced by both modifying ligands and the external environment (*e.g.*, pH and ionic strength). These charge characteristics are characterized by the zeta potential, which is measured from the outer plane of the fluidic layer bound to the liposome and is typically calculated based on electrophoretic mobility.<sup>51,52</sup>

The zeta potential can be measured using techniques such as LDE or capillary electrophoresis. These methods involve laser irradiation, electrophoretic mobility measurement, and Henry's equation calculation. A high zeta potential (absolute value  $>30$  mV) indicates strong electrostatic repulsion between liposomes, preventing aggregation and maintaining the suspension

**Table 2** Key characterization parameters, analytical techniques, and assay standards for liposomal formulations<sup>a</sup>

Characterization parameter	Analytical techniques	Assay standards
Size PDI	DLS, NTA, TEM DLS, NTA	50–200 nm is suitable for delivery Low PDI ( $<0.3$ ) indicates high uniformity, while $>0.3$ may have multiple particle size distribution peaks that affect stability
Zeta potential	LDE, capillary electrophoresis	High zeta potential (absolute value $>30$ mV) indicates strong electrostatic repulsion
Shape Encapsulation efficiency	TEM, cryo-TEM, AFM UV-Vis, HPLC, LC-MS/GC-MS	Uniform morphology High encapsulation efficiency means strong drug loading capacity
Drug release	UV-Vis, HPLC, LC-MS/GC-MS	Release rate needs to be matched with the administration method

<sup>a</sup> DLS = dynamic light scattering, TEM = transmission electron microscopy, NTA = nanoparticle tracking analysis, LDE = laser Doppler electrophoresis, cryo-TEM = cryo-transmission electron microscopy, AFM = atomic force microscopy, HPLC = high-performance liquid chromatography, UV-Vis = ultraviolet-visible spectroscopy, LC-MS/GC-MS = liquid chromatography-mass spectrometry/gas chromatography-mass spectrometry.





stability. In contrast, a low zeta potential (absolute value <30 mV) or uncharged liposomes are prone to aggregation due to van der Waals forces.<sup>53</sup>

### 3.3 Shape

The morphological features of liposomes are critical parameters for their characterization and optimization, given that they directly affect their physicochemical properties and functions. The three commonly used techniques for morphological analysis are TEM, cryo-TEM, and AFM, each with distinct advantages and limitations.

TEM provides high-resolution two-dimensional images of liposomes but involves complex sample preparation, which may introduce artifacts. Cryo-TEM preserves the natural state of liposomes by rapidly freezing samples, enabling more accurate morphological analysis; however, it is expensive due to high equipment costs and is less effective for larger particles. AFM offers three-dimensional morphological information and allows direct observation of liposomes in their natural environment without extensive sample processing, making it a rapid and non-invasive technique.

### 3.4 Encapsulation efficiency

The encapsulation efficiency is a key parameter for evaluating the drug delivery performance of liposomes, which is defined as the percentage of drug encapsulated within liposomes relative to the total amount of drug used. A high EE (close to 100%) indicates that more drug is effectively encapsulated, thereby improving the therapeutic efficacy, while reducing drug waste and side effects.

To determine EE, the encapsulated drug must first be separated from the free drug using techniques such as centrifugation and dialysis. Subsequently, the amount of encapsulated drug is quantified either indirectly (by measuring the free drug concentration and calculating the difference) or directly (by disrupting the liposomes and quantifying the released drug). The commonly used analytical techniques for drug quantification include UV-Vis, HPLC, and LC-MS/GC-MS.

### 3.5 Drug release

Drug release from liposomes is a critical characteristic of their role as drug delivery systems, directly influencing their therapeutic efficacy and clinical applications. The drug release behavior is typically characterized through *in vitro* release experiments, which are designed to simulate the release kinetics *in vivo*. In these experiments, liposomes are placed in a dialysis bag with a specific molecular weight cutoff (MWCO) to retain the liposomes, while allowing the drug to freely penetrate. The release medium, usually buffered saline at pH 7.4, mimics the physiological environment. Experiments are conducted at 37 °C with continuous agitation to mimic *in vivo* conditions. At defined time points, samples are collected, and the drug concentration is quantified using techniques such as UV-Vis and HPLC. Subsequently, the cumulative release curves are plotted to assess the rate and total amount of drug released.

The rate of drug release is influenced by several factors, including liposome composition, membrane rigidity, drug properties, and external conditions (e.g., pH and ionic strength). For instance, increasing the cholesterol content enhances the membrane rigidity, delaying drug release, while pH-sensitive liposomes enable targeted release in specific pH environments. Although *in vitro* release experiments provide valuable insights, *in vivo* release may be further influenced by factors such as hemodilution, plasma protein binding, and cellular uptake.

## 4. Functionalization strategies

### 4.1 “Stealth” liposome

Stealth liposomes, also known as long-circulating liposomes, are designed by coating the liposomal membrane surface with biocompatible hydrophilic polymers such as polyethylene glycol (PEG), making them invisible to phagocytes.<sup>54</sup> Conventional liposomes have a short blood circulation half-life and are rapidly cleared by the mononuclear phagocyte system (MPS).<sup>55,56</sup> PEGylation addresses this limitation by creating a dense hydration layer around the liposomes in an aqueous environment, which generates a steric hindrance effect.<sup>57,58</sup> This steric hindrance reduces the adsorption of serum proteins and minimizes the recognition by phagocytic cells, effectively preventing the rapid clearance of liposomes. Additionally, PEGylation improves the stability of conventional liposomes, making them more effective for drug delivery applications. Research has demonstrated that the length and surface density of PEG chains are critical factors influencing the circulation time of liposomes.<sup>59</sup> Increasing the PEG concentration from 5% to 10% further enhances the stealth properties of liposomes.<sup>60</sup>

### 4.2 Targeted liposomes

Targeting strategies in drug delivery are primarily categorized into passive and active targeting. Passive targeting leverages the enhanced permeability and retention (EPR) effect, which exploits the abnormally leaky vasculature and impaired lymphatic drainage in tumor tissues. This allows nanoscale liposomes (ranging from 10 to 500 nm) to selectively accumulate at the tumor site.<sup>61,62</sup> However, the EPR effect has limitations due to its heterogeneity. For instance, the vascular permeability varies across different tumor types, developmental stages, and regions within the same tumor. Additionally, challenges such as uneven drug distribution and toxicity to normal tissues have hindered its widespread application in tumor therapy.<sup>63</sup> Thus, to address these limitations, researchers are actively exploring active targeting strategies. Active targeting involves conjugating small molecule ligands, peptides, or monoclonal antibodies to the surface of liposomes.<sup>64,65</sup> These modifications enable liposomes to specifically recognize and bind to receptors overexpressed on target cells.<sup>66</sup> For example, folate receptors, epidermal growth factor receptor and transferrin receptors are commonly overexpressed in various cancer types, and liposomes modified with their corresponding ligands have demonstrated significantly improved tumor-targeting



efficiency.<sup>67–70</sup> Furthermore, liposomes can be modified with mitochondria-targeting ligands such as triphenylphosphine (TPP).<sup>71</sup> This expands their targeting capability to induce apoptosis in drug-resistant tumor cells at the mitochondrial level, effectively overcoming multidrug resistance in tumors.

### 4.3 Stimuli-responsive liposomes

**4.3.1 pH-responsive liposomes.** pH-responsive liposomes are designed to achieve targeted drug release in response to changes in environmental pH, significantly enhancing the therapeutic efficacy, while minimizing side effects. These liposomes remain stable under normal physiological conditions (pH ~7.4) but undergo structural destabilization when exposed to acidic environments (*e.g.*, pH <6 in tumor tissues or inflammatory regions), leading to the release of the encapsulated drugs. This responsive mechanism relies on the chemical composition of the lipid bilayer, particularly the incorporation of pH-sensitive molecules (such as phosphatidylethanolamine, PE) or ligands (such as pH-responsive peptides). Under acidic conditions, these components become protonated, disrupting the membrane integrity and triggering drug release.<sup>72,73</sup> pH-responsive liposomes exhibit significant advantages in anti-tumor therapy by leveraging the acidic nature of the tumor microenvironment. They enable precise drug release and highly efficient tumor cell killing, offering a promising strategy for targeted cancer treatment.

**4.3.2 Temperature-sensitive liposomes.** Temperature-sensitive liposomes can target drug release in response to changes in external temperature. These liposomes remain stable at normal body temperature (37 °C), but when the temperature rises to a specific threshold (typically around 42 °C), their lipid membranes become more fluid, leading to enhanced permeability and subsequent release of the encapsulated drug.<sup>74</sup> Conventional temperature-sensitive liposomes are typically composed of lipids with higher gel-liquid phase transition temperatures ( $T_m$ ), such as dipalmitoylphosphatidylcholine (DPPC) and distearoylphosphatidylethanolamine-PEG<sub>2000</sub> (DSPE-PEG<sub>2000</sub>). Mixing lipids with different phase transition temperatures optimizes the thermal responsiveness of liposomes, enhancing the drug release efficiency.

However, the elevated thermal dose required for conventional thermosensitive liposomes may cause damage to healthy tissues. Thus, to address this limitation, a new generation of temperature-responsive liposomes incorporates materials such as temperature-sensitive polymers and lysophospholipid, which lower the phase transition temperature, while enabling rapid drug release.<sup>75</sup> Additionally, technologies such as localized infrared heating allow precise control of the tumor tissue temperature, triggering the structural destabilization of liposomes and the release of drugs.<sup>76</sup> This approach improves both the targeting and safety of therapeutic interventions.

## 5. Chemotherapy

In the treatment of early BC, prophylactic intravesical infusion of chemotherapy drugs after TURBT is the routine means for

clinicians to prevent recurrence. In locally advanced and metastatic BC patients, cisplatin-based chemotherapy may have superior efficacy compared to other chemotherapeutic agents.<sup>77</sup> However, repeated intravesical instillation with cisplatin may cause chemical cystitis, anaphylactic reactions and other side effects; as a result, the prior clinical trial for the usage of cisplatin in NMIBC was stopped due to these side effects.<sup>78</sup> von der Maase *et al.* evaluated cisplatin-loaded and PEG-coated liposomal formulations for BC treatment, demonstrating a significant enhancement in the cytotoxicity of cisplatin, with a 2.4- and 1.9-fold increased efficacy at 24 and 48 h, respectively. In *in vivo* evaluations of an orthotopic BC model in rats, a 4.8-fold reduction in tumor volume and a 3.3-fold decrease in toxicity effects were observed through PLCispt treatment compared to free cisplatin. PEGylated liposomes offer a promising approach to enhance the anticancer effects, while reducing the toxicity of cisplatin in normal tissue.<sup>22</sup>

Lv *et al.* developed an intravesical administration route of multi-responsive delivery system (FA-TMLs@MNP-GNR-DOX) using a microfluidic hybrid chip encapsulating components including MNPs (magnetic nanoparticles), GNRs (gold nanorods), and DOX in folic acid-modified thermosensitive liposomes. The liposome delivery system was enriched by MNPs in response to an external magnetic field to the diseased area. Then, FA-TMLs could more precisely release DOX into tumor cells by recognizing specific receptors on the surface of tumor cells without causing damage to normal tissues. When the incubation temperature increased to 45 °C, 90.1% of the drug was released after 30 min. However, only about 52.2% of DOX was released from FA-TMLs@MNP-GNR-DOX after 24 h incubation at 24 °C. GNRs could not only realize the release of DOX wrapped by photo-controlled changes in the structure of the liposome but also enhanced the therapeutic effect through thermodynamic therapy and chemotherapy owing to their significant photothermal effect. After 980 nm light treatment, 85.4% of the drug was released after 30 min, resulting in a decrease in cell survival from 29.7% ± 3.5% to 7.4% ± 3.6%. When controlling the conditions for which the irradiation power was 0.5 W cm<sup>-2</sup> and GNRs concentration was 150 μM, the temperature was kept at about 50 °C. In this study, through the synergistic effect of heat, gold nanoparticles, and magnetic nanoparticles, the precision of the drug delivery system was enhanced, the drug release time was shortened, and the drug delivery efficiency was improved, which provides a good idea for multi-response synergistic drug delivery systems. However, this study lacked data support from animal experiments, and future work can focus on establishing an *in situ* model of bladder cancer and quantifying the spatial and temporal distribution of the magnetic/photo-thermal targeting properties *in vivo*.<sup>21</sup>

Kamoun *et al.* developed an antibody-directed nano-therapeutic drug, EphA2-ILS-DTXp, designed to target the EphA2 receptor. This formulation encapsulated a hydrolysis-sensitive docetaxel prodrug (DTXp). EphA2 is a member of the Ephrin/Eph receptor family, which plays a crucial role in cell proliferation, differentiation, and migration. Immunohistochemical analysis of 177 human bladder cancer samples revealed that EphA2 was present in 80% to 100% of cases and



was significantly correlated with shorter patient survival. At an equivalent toxic dose, EphA2-ILS-DTXp demonstrated superior antitumor activity compared to free DTX, effectively inhibiting tumor growth and promoting tumor shrinkage in four xenograft models derived from EphA2-positive bladder cancer patients. Furthermore, when combined with gemcitabine, EphA2-ILS-DTXp showed greater efficacy in controlling tumor growth than either monotherapy or free DTX combined with gemcitabine. Currently, EphA2-ILS-DTXp (MM-310) is under evaluation in a clinical trial (NCT03076372).<sup>79</sup>

In addition to traditional chemotherapeutic agents, several natural compounds have also been reported for use in chemotherapy. One compound is  $\beta$ -elemene ( $\beta$ -E) which is extracted from the herb *Curcuma wenyujin*.<sup>80</sup> Based on its antitumor properties, Zhai *et al.* developed a polyethylene glycolylated  $\beta$ -elemene liposome (PEG-Lipo- $\beta$ -E) for targeted delivery to BC cells that overexpress the urokinase plasminogen activator receptor (uPAR). The study protocol improved the stability, sustained release, and enhanced bioavailability compared to conventional  $\beta$ -elemene injections. *In vivo*, the combination of PEG-Lipo- $\beta$ -E and cisplatin exhibited a synergistic effect, significantly inhibiting tumor growth and inducing apoptosis in BC cells without remarkable toxicity to major organs.<sup>81</sup> In the same year, they expanded on this research, utilizing an amino-terminal fragment (ATF) peptide-functionalized  $\beta$ -elemene nanostructured lipid carrier (ATF24-PEG-Lipo- $\beta$ -E), which further enhanced BC treatment combined with cisplatin. Specifically, it exerted a synergistic effect, enhancing cellular apoptosis and inducing cell cycle arrest at the G2/M phase *via* caspase-dependent and Cdc25C/Cdc2/cyclin B1 pathways. *In vivo* studies further confirmed that the targeted liposomes effectively inhibited tumor growth and induced apoptosis in BC cells. ATF24-PEG-Lipo- $\beta$ -E exhibited small and uniform particle sizes, high drug loading capacity and entrapment efficiency, and sustained drug release properties. It demonstrated superior targeting efficiency and cytotoxicity compared to PEG-Lipo- $\beta$ -E.<sup>82</sup>

Curcumin (CUR) is a lipophilic polyphenol isolated from the rhizome of the turmeric (*Curcuma longa*). It has been shown to exhibit anti-infectious, antioxidant, anti-inflammatory, and anticarcinogenic properties. However, due to its poor bioavailability, restricted cellular uptake, and rapid metabolic degradation, its therapeutic potential is exceptionally limited *in vivo*.<sup>83–85</sup> Gholami *et al.* reported the liposomal encapsulation of curcumin with soybean phosphatidylcholine (SPC) and hydrogenated SPC (HSPC), a strategy that significantly improved the therapeutic efficacy of curcumin. Compared with free curcumin, the liposome-encapsulated curcumin exhibited greater stability under pH changes from alkaline to acidic ( $p < 0.001$ ) and maintained stability for 14 weeks when stored at 4 °C. Moreover, liposome encapsulation enabled the sustained release of curcumin. Additionally, this method significantly enhanced the cellular uptake of curcumin and its cytotoxic effects against HTB9 bladder cancer cells.<sup>86</sup>

Piwowarczyk *et al.* evaluated the stability of liposomal formulations containing CUR, epigallocatechin gallate phosphate (pEGCG), and their combination, respectively, and also

assessed their anticancer potential against bladder and prostate cancer cell lines. The results revealed that the encapsulation method improved the stability, with only a slight increase in particle size from 130 nm to 146 nm over 28 days. The combined liposomal formulation demonstrated selective anticancer effects and strong cytotoxicity, particularly against the BC cell line (5637), with an  $IC_{50}$  value of  $15.33 \pm 2.03 \mu\text{M}$ . Notably, the combination of CUR and pEGCG in liposomes exhibited a synergistic effect, which demonstrated greater stability compared to their individual forms. Curcumin primarily contributed to the anticancer activity, while pEGCG enhanced the stability. When co-encapsulated, CUR maintained a high encapsulation efficiency of 91.51% and the encapsulation efficiency of pEGCG increased to 76.84%, indicating a beneficial interaction when delivered together in liposomes. This liposomal combination offers a promising therapeutic strategy that may overcome the issues of instability and poor bioavailability.<sup>87</sup>

### 5.1 Chemotherapy combined with hyperthermia

Thermosensitive liposomes (TSLs) have been a prominent focus in tumor-targeted chemotherapeutics. The circulation of TSLs through the vasculature of a heated tumor triggers the release of liposomal drugs.<sup>88,89</sup> Furthermore, hyperthermia (HT) ( $42 \text{ }^{\circ}\text{C} \pm 2 \text{ }^{\circ}\text{C}$ ) enhances the effects of chemotherapy by improving the tissue penetration and stimulating an anti-tumor immune response.<sup>90–92</sup> As early as 2017, a study evaluated the effectiveness of lyso-thermosensitive liposomal doxorubicin (LTLD, ThermoDox®) in combination with regional mild HT for BC treatment. Compared to intravenous (IV) DOX with HT or IV LTLD without HT (LTLD – HT), the IV LTLD with HT (LTLD + HT) resulted in the significantly higher accumulation and distribution of DOX within the bladder wall.<sup>93</sup>

Recently, TSL using 1,2-dipalmitoyl-*sn*-glycero-3-phosphoglyceroglycerol (DPPG<sub>2</sub>) as a lipid excipient showed promising results in the treatment of MIBC in different animal models (pigs and rats) when encapsulating DOX (DPPG<sub>2</sub>-TSL-DOX) and combined with regional HT. IV DPPG<sub>2</sub>-TSL-DOX with HT significantly increased the DOX concentrations and distribution compared to conventional intravenous and intravesical DOX application, with reduced DOX accumulation in the heart and kidneys.<sup>24,25</sup> These studies confirmed that TSLs combined with HT not only improved the drug delivery targeting, but also increased the penetration and concentration of chemotherapy drugs in the bladder wall. Thus, TSLs encapsulating chemotherapeutics may play a role in the treatment of BC in the future.

### 5.2 Chemotherapy combined with radiotherapy

In recent years, combining chemotherapy with radiation therapy has been suggested by researchers as a method to enhance the efficacy of radiotherapy and reduce side effects. Panteliadou *et al.* explored the impact of combining liposomal doxorubicin (LDox) with hypofractionated accelerated radiotherapy (HypoARC) in treating MIBC. Eighty-two patients received HypoARC, and forty-one out of eighty-two patients were treated with LDox concurrently. This study revealed





a significantly improved 3 year survival rate in T2-4 stage patients receiving LDox, with rates of 72.1% vs. 58.7% ( $P = 0.04$ ). Also, LDox was free of haematological toxicity, only a slight side effect observed in 5 out of 41 patients. However, no significant differences were observed in the other evaluation metrics. This study confirmed that combining chemotherapy with radiotherapy can enhance the therapeutic effect to a certain extent, but further exploration is needed. For instance, developing new radiotherapy sensitizers or improving the targeting of existing ones (Table 3).<sup>94</sup>

## 6. Immunotherapy

Since its initial documentation in 1976, a growing body of clinical evidence has supported the use of intravesical *Bacillus Calmette–Guérin* (BCG) therapy as the standard treatment for intermediate- and high-risk NMIBC.<sup>95</sup> Upon the administration of BCG, the fibronectin attachment protein (FAP) located on the surface of the mycobacterium binds with fibronectin present on urothelial cells, facilitating BCG adhesion to the urothelium.<sup>96–98</sup> Subsequently, BC cells internalize BCG through micropinocytosis, a process that is much more difficult for normal urothelial cells to undergo.<sup>99–101</sup> This internalization triggers the activation of various immune cells, leading to both innate and adaptive immune responses.<sup>102–104</sup> Furthermore, BCG can induce apoptosis in BC cells directly<sup>105</sup> and promote cell death through oxidative stress.<sup>106–108</sup> However, this therapy is often discontinued because of its side effects, including significant urinary symptoms, systemic infections, and sepsis.<sup>109</sup> In addition, BCG-relapse and BCG-refractory have severely limited its application. As a result, researchers have been investigating safer and more effective alternative schemes, including combining BCG with interferon, lowering the BCG dose, and administering prophylactic tuberculostatic agents. Several studies successfully reduced the side effects of BCG therapy and prolonged the BCG exposure time in the bladder *via* nanotechnologies.

For instance, Ma and colleagues formulated a glutathione (GSH)-responsive lipophilic oxaliplatin prodrug and incorporated it in cationic liposomes (LRO) modified with a cell-penetrating peptide to enhance the penetration and drug release in bladder tumor tissues. Then, LRO and a low-dose BCG were co-delivered in viscous CS solution (LRO-BCG/CS) to prolong the retention time of the drugs and enhance their permeability across the bladder urothelium. Oxaliplatin triggered immunogenic cell death and its combination with BCG simultaneously further activated the systemic anti-tumor immune response. In an orthotopic bladder tumor model, LRO-BCG/CS inhibited tumor growth greatly, as evidenced by the average tumor volume in the LRO-BCG/CS group, which was 4.2-, 5.0- and 5.3-fold smaller than that in the LRO/CS, OXA/CS, and BCG groups, respectively. At relatively low doses of oxaliplatin and BCG, LRO-BCG/CS showed superior anti-tumor effects and prolonged the survival time of tumor-bearing mice. Importantly, this combination of chemotherapy with immunotherapy showed negligible side effects, providing

a promising and well-tolerated treatment strategy for BC patients.<sup>23</sup>

The BCG cell wall skeleton (BCG-CWS) is the active immunoadjuvant component of BCG and can potentially replace live BCG.<sup>110</sup> However, the clinical application of BCG-CWS is limited due to its poor solubility and low uptake by cancer cells. Thus, to address these challenges, researchers have employed octaarginine-modified liposomes (R8-liposomes) as a delivery system to enhance the intracellular transport of BCG-CW into the cytoplasm of BC cells. This approach improves the solubility and stability of BCG-CW, increasing the susceptibility of cancer cells to lysis by lymphokine-activated killer cells, and significantly enhancing its immunotherapeutic efficacy.<sup>111,112</sup>

Whang *et al.* developed a nanoparticulate system using the liposomal encapsulation of BCG-CWS, functionalized with folic acid (FA) for targeting and Pep-1 peptide (Pep1) for cell penetration. The liposomes were produced *via* a modified emulsification-solvent evaporation method, resulting in a particle size below 200 nm and an encapsulation efficiency of 60%. This system enhanced the uptake of BCG-CWS in BC cells and improved the immunoactivity, as shown by the increased cytokine production and THP-1 cell migration. *In vivo* studies demonstrated that FA- and Pep1-modified dual ligand-functionalized liposomes effectively inhibited tumor growth in mice bearing MBT2 tumors, surpassing single-ligand systems. Immunohistochemistry confirmed the increase in IL-6 production and CD4<sup>+</sup> T-cell infiltration, indicating enhanced antitumor immunity.<sup>113</sup>

In another study, liposome-encapsulated BCG-CWS nanoparticles (CWS-Nano-CL) were developed using liposome evaporation *via* an emulsified lipid (LEEL) method to prevent aggregation issues and improve their internalization. The resulting BCG-CWS nanoparticles had a particle size of approximately 180 nm. *In vitro* experiments demonstrated the increased inhibition of BC cells, CWS-Nano-CL activated AMP-activated protein kinase (AMPK), and the mammalian target of rapamycin (mTOR), leading to increased autophagy and apoptosis through the production of reactive oxygen species (ROS) and induction of endoplasmic reticulum (ER) stress. In orthotopic bladder tumor models, significant tumor regression was observed without the formation of hydrophobic aggregates of CWS. Furthermore, coating CWS Nano CL with chitosan enhanced the adhesion of the nanoparticles on the surface of the bladder mucosa, increased the local concentration of drugs, and further optimized the therapeutic effect.<sup>114</sup>

Shiga *et al.* engineered cationic liposomes, Lip-TDM, containing trehalose 6,6'-dimycolate (TDM) purified from *Mycobacterium bovis* BCG Connaught. TDM has been shown to have strong immunostimulatory activity but would induce granuloma formation.<sup>115</sup> Lip-TDM could minimize the virulence of TDM, and it exhibited an antitumor effect comparable to or greater than that of BCG and fewer side effects such as weight loss and granuloma formation, which was proven in mouse models of BC, colon cancer, and melanoma. In mice lacking CD8<sup>+</sup> T cells and those with the genetic deletion of macrophage-inducible C-type lectin (Mincle), the antitumor effect of Lip-TDM was absent, which means that the anti-tumor effect of







Table 3 Summary and characteristics of liposomal formulations for bladder cancer chemotherapy<sup>a</sup>

Composite name	Synthetic components	Functionalization	Size (nm)	Therapeutic agents	Advantages	Administration method
PLCispt <sup>22</sup>	Lecithin, cholesterol, PEG	PEGylation	251 ± 12 nm	Cisplatin	- Increased drug efficacy - Reduced toxicity	Intraperitoneal injection
FA-TMLs@MNP-GNR-DOX <sup>21</sup>	DPPC, cholesterol, DSPE-PEG <sub>2000</sub>	Folate receptor-targeted, magnetic and photothermal-responsive, thermal liposomes	230 nm	DOX	- High encapsulation efficiency - Multi-responsive to stimulus - Targeted delivery to folate-receptor-positive cells	Intravenous injection
EphA2-IL-DTXp <sup>79</sup>	EPC, cholesterol, PEG-DSG	EphA2 targeted liposomes	113.6 nm	DTXp	- Controlled drug release - Targeted delivery to EphA2-expressing cancer cells - Enhanced tumor-specific accumulation and reduced systemic toxicity - Significant tumor regression in PDX models - Synergistic effect when combined with gemcitabine	Intravenous injection
PEG-Lipo-β-E <sup>81</sup>	SPC, DSPE-PEG <sub>2000</sub>	PEGylation	83.31 ± 0.181 nm	β-E	- High entrapment efficiency - Enhanced anticancer effects, prolonged circulation time, and reduced clearance - No significant toxicity to major organs	Intravenous injection
ATF <sub>24</sub> -PEG-Lipo-β-E <sup>82</sup>	SPC, DSPE-PEG <sub>2000</sub>	Targeted to uPAR	79 nm	β-E, cisplatin	- Enhanced tumor targeting of uPAR-expressing cells - Synergistic effect with cisplatin in inhibiting tumor growth and inducing apoptosis	Intravenous injection
SPC/HSPC liposomes <sup>86</sup>	SPC/HSPC, cholesterol	—	127.46 ± 1.1 nm/ 136.1 ± 0.2 nm	Curcumin	- Sustained drug release behavior - Enhanced cellular uptake - Increased stability and bioavailability - Selective cytotoxicity against cancer cells	—
CUR + pEGCG/POPC <sup>87</sup>	POPC, DOTAP	—	123.3 ± 41.8 nm	Curcumin and pEGCG	- High encapsulation efficiency - Enhanced stability, increased anticancer potential, and protection against degradation - Controlled release and low toxicity to normal cells	—
L/TLD-DOX <sup>93</sup>	—	Lyso-thermosensitive liposome	—	DOX	- Enhanced doxorubicin accumulation in the bladder wall when combined with hyperthermia - Targeted drug release triggered by mild hyperthermia - Minimal systemic toxicity and increased local drug delivery	Intravenous with hyperthermia



Table 3 (Contd.)

Composite name	Synthetic components	Functionalization	Size (nm)	Therapeutic agents	Advantages	Administration method
DPPG <sub>2</sub> -TSL-DOX <sup>24,25</sup>	—	Thermosensitive liposome	110–130 nm	DOX	- Enhanced doxorubicin accumulation in the bladder wall - Reduced toxicity in heart and kidneys - Homogeneous drug distribution in bladder wall layers - Improved survival in invasive bladder cancer patients - Reduced systemic toxicity	Intravenous with hyperthermia
LDox <sup>94</sup>	—	—	—	DOX		Intravenous with HypoARC

<sup>a</sup> SPC, soybean phosphatidylcholine; HSPC, hydrogenated soybean phosphatidylcholine; POPC, 1-palmitoyl-2-oleoyl-*sn*-glycero-3-phosphocholine; DOTAP, 1,2-dioleoyl-3-trimethylammonium-propane; EPC, egg sphingomyelin; PEG-DSG, polyethylene glycol-distearoyl glycerol; DPPC, 1,2-dipalmitoyl-*sn*-glycero-3-phosphocholine.

Lip-TDM is achieved by enhancing the activation of CD8<sup>+</sup> T cells in the tumor microenvironment and inducing the activation of DCs. Mincle is an important receptor for the anti-tumor effect of Lip-TDM.<sup>116</sup>

Mycolic acid (MA), recognized as the major lipid in the BCG cell wall, is thought to be a key component of its immunogenic properties. Yoshino and team developed cationic liposomes that encapsulate three distinct subclasses of MA,  $\alpha$ , keto, and methoxy, using the dendron-bearing lipid D22. Among them, Lip-kMA demonstrated particularly potent antitumor activity in two murine syngeneic graft models involving the murine BC cell lines MB49 and MBT-2, surpassing the effects observed with Lip-aMA and Lip-mMA, which contained  $\alpha$ -MA and methoxy-MA, respectively. Lip-kMA triggered a strong antitumor immune response driven by T cells. Histological examinations showed a marked increase in CD8<sup>+</sup> lymphocytes infiltrating the tumors treated with Lip-kMA compared to that receiving the control treatments. The antitumor effects of Lip-kMA were significantly diminished in athymic nude mice, which lacked T cells, while some antitumor effects were still evident in beige mice, which were deficient in natural killer activity. These findings offer valuable insights into the immunogenicity of lipids and the underlying mechanisms of BCG-based immunotherapy.<sup>117</sup>

Samaddar *et al.* presented a targeted immunotherapeutic system integrating active targeting, pH-sensitivity, and CpG oligonucleotide delivery, optimized for interaction with the bladder tumor microenvironment. A critical feature of the fibronectin attachment protein (FAP) is its RWFV peptide sequence, which is essential for BCG internalization *via* binding to fibronectin (FBN) within the tumor microenvironment. This system was composed of pH-sensitive lipid nanoparticles (LNPs) incorporating the RWFV peptide and cholesterol hemisuccinate (CHEMS) for targeted delivery. In MB49 bladder tumor cells, the fluorescence intensity of the targeted LNPs was 200% higher than that of the non-targeted LNPs, indicating that the targeted LNPs have a stronger binding affinity for cells with a fibronectin-enriched extracellular matrix. pH-sensitive LNP formulations led to the more efficient release of their therapeutic agent. Upon endosomal acidification, the targeted pH-sensitivity LNPs enhanced the expression of CD83, CD86, MHC class II molecules, and TNF- $\alpha$ , resulting in a stronger immune response.<sup>118</sup>

### 6.1 Other immunotherapy

In recent years, various checkpoint inhibitors such as PD-L1/PD1, and CTLA-4 have been developed for BC treatment. However, the low responsiveness of checkpoint blockade immunotherapy (CBI) limits its efficacy in BC.<sup>15</sup> Ferroptosis has shown promise in enhancing the CBI responsiveness by inducing immunogenic cell death (ICD). Ding *et al.* developed a mitochondrial-targeted liposome (BQR@MLipo) loaded with brequinar to enhance mitochondrial-related ferroptosis in BC. *In vivo* studies showed that BQR@MLipo significantly accumulates within bladder tumors, effectively promoting the infiltration of CD8<sup>+</sup> T cells into the tumor microenvironment.

This formulation substantially improved the delivery efficiency of brequinar, inducing mitochondrial lipid peroxidation and generating reactive oxygen species (ROS), ultimately triggering ferroptosis in BC cells. This process led to the release of damage-associated molecular patterns (DAMPs) and the activation of the cGAS-STING signaling pathway, contributing to the effective inhibition of bladder tumor growth through CBI (Table 4).<sup>119</sup>

## 7. Gene therapy

Gene therapy delivers therapeutic genes into target cells using viral or non-viral vectors. These vectors can introduce DNA, RNA, or small interfering RNA (siRNA) to regulate, replace, or modify specific gene functions or induce cytotoxic effects. Viral vectors offer high transfection efficiency. However, their production is complex and costly, and they pose safety concerns such as immunogenicity and oncogenicity. Alternatively, cationic liposomes, a type of non-viral vector, are easy to prepare and exhibit high transfection efficiency. They can encapsulate both lipophilic and hydrophilic drugs, making them widely used in gene therapy.

Conventional intravesical BCG therapy generates only a localized immune response and fails to establish long-term systemic immune memory against bladder cancer, which may contribute to late disease progression.<sup>120</sup> Studies have shown that delivering cytokines such as IL-2 and IL-12 to the bladder using cationic liposomes can induce durable tumor-specific immunity and improve the tumor-specific biodistribution.

Horiguchi *et al.* used cationic liposomes composed of DMRIE/DOPE to deliver the IL-2 gene into a mouse *in situ* bladder cancer model *via* bladder perfusion. The results showed that IL-2 transfection was limited to the surface of the bladder tumor cells, while the normal urothelium remained largely untransfected. The mean survival of the IL-2-treated group was significantly longer than that of the control group, with a mean survival of  $43.8 \pm 4.8$  days. By day 21, the tumor volume in the IL-2-treated group was significantly smaller than that in the control group. By day 60, the survival rate in the IL-2 group reached 40% (4/10), while no mice survived in either control group. CTL (cytotoxic T-lymphocyte) response assessment indicated enhanced anti-tumor immunity in the IL-2-treated animals. Additionally, the IL-2-treated group exhibited significant anti-tumor immune responses and successfully resisted tumor recurrence after a second challenge, suggesting that IL-2 therapy not only eliminates existing tumors but also induces immune memory. Only 2 out of 30 experimental mice developed bladder stones, demonstrating good overall tolerability.<sup>121</sup>

Horinaga *et al.* employed the same experimental approach, utilizing DMRIE/DOPE cationic liposomes for gene delivery *via* bladder infusion in a mouse *in situ* bladder cancer model. However, in this study, they replaced the payload with IL-12 and included BCG as a control group to compare their therapeutic effects. The results indicated that the reduction of tumor growth in the IL-12 group was significantly greater than in the BCG group, with tumor inhibition exceeding 80%. Although BCG inhibited tumor growth, it was slightly less effective than IL-12.

Furthermore, the tumor in the IL-12 group exhibited significantly increased infiltration of CD8<sup>+</sup> T cells and NK cells, suggesting that IL-12 effectively enhanced the anti-tumor immune response. Similarly, the BCG group induced an immune response, but with lower T-cell infiltration than the IL-12 group. Additionally, in the secondary tumor challenge assay, the mice in the IL-12 group exhibited a more robust anti-tumor response, indicating that IL-12 induced a durable tumor-specific immune memory. In contrast, the mice in the BCG group still showed tumor growth after the second challenge, suggesting that its immune-protective effect may not be as long-lasting as that of IL-12.<sup>122</sup>

Compared to IL-2, which primarily promoted T-cell proliferation, IL-12 activated a broader immune response involving both T cells and NK cells, suggesting a more comprehensive role in anti-tumor immunity.

Wu *et al.* utilized plasmid vectors to transfect mouse interferon (IFN- $\alpha$ ) and granulocyte macrophage colony-stimulating factor (GM-CSF) genes using cationic liposomes (DOTAP and MBC) as delivery agents. BC cells exhibited a significant reduction in viability following treatment with the liposome-DNA complex. Notably, the proliferation inhibition rate of the tumor cells transfected with IFN- $\alpha$  alone was 37%, which was considerably higher than that observed in cells transfected with GM-CSF alone or in combination with IFN- $\alpha$  and GM-CSF. After intravesical administration of the plasmid-liposome complex, the incidence dropped significantly from 76.9% in the control groups to 15.4–30.8% in the treated groups.<sup>123</sup>

CRISPR-Cas13a is a precise and potent RNA editing tool, offering a promising approach for BC treatment. In a recent study, Fan *et al.* developed a multifunctional liposome system incorporating a CRISPR-Cas13a gene circuit. This system utilizes a multi-level targeting strategy, including hVEGFR2 targeting, a CRISPR sequence driven by a tumor-specific artificial promoter, and a near-infrared light-controlled release mechanism. *In vitro* experiments revealed that this system effectively downregulated VEGFR2, Bcl-2, and survivin gene expression, leading to the significant suppression of BC cell proliferation, migration, and invasion. Furthermore, its light-controlled release properties enhanced the targeted therapeutic effect of the system. *In vivo* studies using a mouse model further confirmed the ability of this system to inhibit tumor growth and promote cell death in BC.<sup>124</sup>

Small interfering RNA (siRNA) is widely used to inhibit oncogene expression by targeting and degrading mRNA. However, its *in vivo* applications face challenges due to its vulnerability to degradation and inability to efficiently penetrate cell membranes because of its negative charge. Thus, to address these issues, cationic liposomes, cationic polymers, and viral vectors are typically employed to protect siRNA and enhance its delivery.<sup>125</sup> Polo-like kinase-1 (PLK-1) is a key regulator of mitotic progression in mammalian cells,<sup>126</sup> and its over-expression is strongly associated with a broad range of human tumors. In particular, high PLK-1 expression in BC is closely linked to tumor progression and poor prognosis.<sup>127–129</sup>

Nogawa *et al.* developed a cationic liposome-based delivery system to deliver polo-like kinase-1 (PLK-1) siRNA. In both UM-





Table 4 Summary and characteristics of liposomal formulations for bladder cancer immunotherapy<sup>a</sup>

Composition name	Synthetic components	Functionalization	Size (nm)	Therapeutic agents	Advantages	Administration method
LRO-BCG/CS <sup>2,3</sup>	DOPC, cholesterol, C <sub>18</sub> -R <sub>6</sub> H <sub>3</sub> , chitosan	Chitosan-coated liposomes	110 nm	Oxaliplatin prodrug, BCG	<ul style="list-style-type: none"><li>- Prolonged retention and enhanced permeability</li><li>- Inhibition tumor growth and increased survival time</li><li>- Reduced systemic toxicity and adverse effects</li><li>- Enhanced delivery and internalization into cancer cells</li><li>- Antitumor effects observed <i>in vivo</i></li><li>- Increased recruitment and activation of immune cells</li></ul>	Intravesical administration
R8-liposome-BCG-CW <sup>111</sup>	EPC, cholesterol, stearylated-octaarginine	—	233 nm	BCG-CWS	<ul style="list-style-type: none"><li>- Reduced adverse effects</li><li>- Enhanced cellular uptake and antitumor activity</li><li>- Maximum tumor growth inhibition</li><li>- Inhibited tumor growth</li><li>- Increased AMPK activation and ROS production</li><li>- Greater efficacy and reduced toxicity</li></ul>	Subcutaneous injection co-injection
CWS-FPL <sup>113</sup>	SPC, cholesterol, DSPE-PEG <sub>2000</sub> -Mal, DSPE-PEG <sub>5000</sub> -Fol	FA-and Pep1-modified liposomes	189.4 ± 0.23 nm	BCG-CWS	<ul style="list-style-type: none"><li>- Reduced adverse effects</li><li>- Enhanced cellular uptake and antitumor activity</li><li>- Maximum tumor growth inhibition</li><li>- Inhibited tumor growth</li><li>- Increased AMPK activation and ROS production</li><li>- Greater efficacy and reduced toxicity</li></ul>	Subcutaneous injection co-injection
CWS-Nano-CL-chitosan <sup>114</sup>	SPC, cholesterol, chitosan	Chitosan-coated liposomes	196.33 ± 0.34 nm	BCG-CWS	<ul style="list-style-type: none"><li>- Reduced adverse effects</li><li>- Enhanced cellular uptake and antitumor activity</li><li>- Maximum tumor growth inhibition</li><li>- Inhibited tumor growth</li><li>- Increased AMPK activation and ROS production</li><li>- Greater efficacy and reduced toxicity</li></ul>	Intravesical administration
Lip-TDM <sup>116</sup>	DOPC, cholesterol, cationic dendron-bearing lipid D22	—	157.2 nm	TDM	<ul style="list-style-type: none"><li>- Enhanced antitumor effects</li><li>- Reduced adverse effects</li><li>- Induced maturation and migration of dendritic cells and activation of CD8<sup>+</sup> T cells</li></ul>	Subcutaneous and intraperitoneal injection
Lip-kMA <sup>117</sup>	DOPC, cholesterol, cationic dendron-bearing lipid D22	—	154.1 nm	MA	<ul style="list-style-type: none"><li>- Strong antitumor activity</li><li>- Induced infiltration of CD8<sup>+</sup> T cells in tumor tissues</li><li>- Enhanced internalized by cancer cells</li></ul>	Subcutaneous injection
RWfV-LNP <sup>118</sup>	DOTAP, DOPE, CHEMS, DSPE-mPEG <sub>2000</sub>	pH-sensitive and targeted liposomes	<70 nm	CpG	<ul style="list-style-type: none"><li>- No observed toxicity <i>in vitro</i></li><li>- Enhanced bladder tumor targeting and cellular uptake</li><li>- pH-sensitive release of cargo</li><li>- Efficient activation of immune cells</li><li>- Induced strong upregulation of CD83, CD86, and MHC II molecules</li></ul>	—
BQR@MLipo <sup>119</sup>	SPC, DSPE-mPEG <sub>2000</sub> , TPP	Mitochondrial targeted liposomes	93.68 ± 1.69 nm	BQR	<ul style="list-style-type: none"><li>- Mitochondria-targeted delivery</li><li>- Enhanced ferroptosis</li><li>- Boosted anti-tumor immunity</li></ul>	Intravenous injection

<sup>a</sup> DOPC, 1,2-dioleoyl-*sn*-glycero-3-phosphocholine; SPC, soy phosphatidylcholine; EPC, egg phosphatidylcholine; DOTAP, 1,2-dioleoyl-3-trimethylammonium-propane; DOPE, 1,2-dioleoyl-*sn*-glycero-3-phosphoethanolamine; CHEMS, cholesteryl hemisuccinate; TPP, hexadecyltriphenylphosphonium bromide.



UC-3LUC cells and an orthotopic murine model, the PLK-1 siRNA/cationic liposome complex suppressed BC growth. In addition, some mice showed complete eradication of cancer cells without severe adverse effects. This study provides the first demonstration of BC growth inhibition in a murine model using intravesical siRNA/cationic liposomes, suggesting a promising non-invasive, targeted therapeutic approach with minimal side effects.<sup>130</sup>

Survivin is an oncogene that can inhibit apoptosis and promote cell proliferation and the over-expression of survivin helps cancer cells to escape from cell cycle checkpoints and inhibits apoptosis.<sup>131,132</sup>

Seth *et al.* developed siRNA constructs (UsiRNA) that contain unlocked nucleobase analogs (UNA) targeting survivin and polo-like kinase-1 (PLK1) genes. The UsiRNAs targeting survivin and PLK1 led to more than a 90% reduction in mRNA levels in three BC cell lines, KU-7-luc, UM-UC3, and T24. In an orthotopic mouse model of BC, intravesical administration of UsiRNA encapsulated in DiLA2 liposomes produced significant, dose-dependent reductions in tumor volume. The PLK1 UsiRNA showed a remarkable 68-fold inhibition of tumor growth at a dose of 1.0 mg kg<sup>-1</sup>, while survivin UsiRNA caused a 10-fold reduction. Furthermore, this study confirmed the RNA interference (RNAi)-mediated gene silencing mechanism by detecting specific cleavage products in bladder tumors. These findings indicate that intravesical delivery of survivin or PLK1 UsiRNA can offer a promising therapeutic approach for treating BC.<sup>133</sup>

Small activating RNA (saRNA) is a type of double-stranded RNA (dsRNA) that induces the expression of specific genes by targeting gene promoters or binding to non-coding regulatory transcripts, a process known as RNA activation (RNAa). This mechanism is similar to RNA interference (RNAi), but unlike RNAi, RNAa promotes gene expression, and thus it can be applied to induce tumor suppressor gene expression, thereby inhibiting tumor growth. Kang *et al.* developed saRNA targeting the p21 gene (dsP21-322-2'F) and formulated it into lipid nanoparticles (LNP), significantly improving its stability in urine. Treatment with LNP-saRNA notably induced p21 expression, leading to cell cycle arrest and apoptosis in BC cells. In an orthotopic BC mouse model, intravesical administration of LNP-dsP21-322-2'F prolonged the survival and resulted in tumor regression or disappearance in 40% of treated mice (Table 5).<sup>134</sup>

## 8. Photodynamic therapy (PDT)

The hollow structure of the bladder facilitates localized treatments, such as photosensitizer-based photodynamic therapy (PDT). Photosensitizers can accumulate in tumor tissues and are sensitive to light. After the activation of oxygen molecules by light, reactive oxygen species (ROS) are generated, and therefore induce cytotoxic effects. The ability of photosensitizers to damage cancer cells was first demonstrated in a rat tumor model.<sup>135</sup> However, these agents, such as ALA (5-aminolevulinic acid) and Photofrin, face certain limitations, including slow metabolism, cutaneous toxicities, and poor tumor specificity.<sup>136</sup>

Despite being one of the first photosensitizers used in clinical PDT, the use of Photofrin is associated with complications such as fibrosis of the bladder wall, reduced bladder capacity, and contracture.<sup>137,138</sup> The therapeutic impact of PDT is contingent upon the availability of a photosensitizing agent, light, and oxygen.<sup>139</sup> The reliance of PDT on oxygen poses another challenge, given that tumors often exhibit hypoxia, which is exacerbated by PDT, reducing its effectiveness. Additionally, PDT can upregulate PD-L1 expression, enabling immune evasion by tumor cells.<sup>140–142</sup> Thus, lipid-based delivery systems for photosensitizers are being developed to improve their tumor specificity and reduce off-target effects. Additionally, combining PDT with immune checkpoint inhibitors offers potential to overcome immune evasion. Research focused on improving the photosensitizer selectivity and addressing tumor hypoxia through advanced delivery systems can greatly enhance the clinical efficacy of PDT in BC.

Titanium dioxide (TiO<sub>2</sub>) is a semiconductor known for its photocatalytic properties, primarily due to its ability to generate reactive oxygen species (ROS) upon UV light absorption. When TiO<sub>2</sub> absorbs UV light, it generates electron-hole pairs, leading to the formation of ROS such as hydroxyl radicals and superoxide anions. Consequently, these ROS can induce strong oxidative stress, potentially inhibiting malignant cell growth by damaging cellular components. Chihara and team observed that when TiO<sub>2</sub> was delivered into cancer cells using liposomes, and subsequently exposed to UVA light (320–400 nm), it triggered a heightened oxidative response and potent anti-tumor activity. Their findings suggest that TiO<sub>2</sub> encapsulated in liposomes (LT) may offer superior efficacy in combating BC compared to its uncoated form.<sup>143</sup>

Annelies S. L. Derycke and colleagues developed a targeted PDT for superficial BC. They encapsulated the photosensitizer ALPcS<sub>4</sub> in transferrin-conjugated liposomes, leveraging the overexpression of transferrin receptors on bladder transitional-cell carcinoma cells to achieve tumor-selective accumulation of the phthalocyanine photosensitizer. *In vitro* experiments showed that TF-Lip-ALPcS<sub>4</sub> demonstrated high cellular uptake and enhanced photocytotoxicity against BC cells compared to non-targeted formulations. *In vivo*, it was found that the glycocalyx layer may hinder the accumulation of TF-Lip-ALPcS<sub>4</sub> in the tumor. After chondroitinase ABC pretreatment, the targeting of TF-Lip-ALPcS<sub>4</sub> in the bladder tumor of rats was significantly enhanced (Table 6).<sup>144</sup>

## 9. Other functionalized liposomes for bladder cancer therapy

Functional liposomes can achieve precise drug release in response to varying microenvironments or external stimuli through targeted modifications or responsive designs, offering distinct therapeutic advantages over conventional liposomes. A key strategy for modifying liposomes involves developing formulations that enable controlled drug release in response to specific physicochemical or biochemical triggers, referred to as stimuli-responsive liposomes. These drug delivery systems





**Table 5** Summary and characteristics of liposomal formulations for bladder cancer gene therapy<sup>a</sup>

Composition name	Synthetic components	Functionalization	Size (nm)	Therapeutic agents	Advantages	Administration method
IL-2 lipoplex <sup>121</sup>	DMRIE, DOPE	—	—	IL-2 gene	<ul style="list-style-type: none"> <li>- Enhanced IL-2 gene and antitumor effect</li> <li>- Induced tumor-specific CTL responses</li> <li>- Generated long-lasting tumor-specific immunologic memory</li> <li>- Improved survival rate and tumor suppression</li> </ul>	Intravesical administration
IL-12 lipoplex <sup>122</sup>	DMRIE, DOPE	—	—	IL-12 gene	<ul style="list-style-type: none"> <li>- Induced antitumor immunity and prolonged survival</li> <li>- Generated long-lasting tumor-specific immunologic memory</li> <li>- Superior to BCG therapy in terms of tumor-specific immune response</li> </ul>	Intravesical administration
IFN-GM-CSF <sup>123</sup>	DOTAP, MBC	—	—	IFN- $\alpha$ , GM-CSF	<ul style="list-style-type: none"> <li>- High transfection efficiency</li> <li>- Enhanced cytokine expression</li> <li>- Significant tumor inhibition</li> </ul>	Intravesical administration
CRISPR-Cas13a/liposome system <sup>124</sup>	DPPC, cholesterol, DOTAP, DSPE-PEG <sub>2000</sub> , DSPE-PEG <sub>2000</sub> -Mal	Near-infrared sensitive and hVEGFR2 targeted liposomes	855 $\pm$ 127 nm	CRISPR-Cas13a	<ul style="list-style-type: none"> <li>- Tumor targeting <i>via</i> hVEGFR2 receptor</li> <li>- Near-infrared controlled release</li> </ul>	Intravesical administration
siRNA/cationic liposomes <sup>13,0</sup>	—	—	—	PLK-1 siRNA	<ul style="list-style-type: none"> <li>- Enhanced delivery</li> <li>- Inhibition of PLK-1 expression</li> <li>- Prevention of bladder cancer growth</li> </ul>	Intravesical administration
DiLA <sup>2</sup> -formulated UsiRNAs <sup>133</sup>	C18:1-norarg-C16, cholesterol, CHEMS, DMPE-PEG <sub>2000</sub>	Survivin and PLK1 targeted liposomes	125 nm	Survivin and PLK1 UsiRNA	<ul style="list-style-type: none"> <li>- Induction of apoptosis</li> <li>- High encapsulation efficiency</li> <li>- Sustained RNAi-mediated activity</li> </ul>	Intravesical administration
LNP-dsP21-322-2'F <sup>134</sup>	DLin KC2-DMA, DSPC, PEG-DMG, cholesterol	—	—	dsP21-322-2'F	<ul style="list-style-type: none"> <li>- Significant tumor reduction</li> <li>- Enhanced RNA stability</li> <li>- Induction of p21 expression</li> <li>- Enhanced tumor inhibition and apoptosis</li> </ul>	Intravesical administration

<sup>a</sup> DMRIE, 1,2-dimyristyl-3-trimethylammoniumethyl sulfatate; MBC, methyl- $\beta$ -cyclodextrin-solubilized cholesterol; DPPC, 1,3-bis(sn-3'-phosphatidyl)-sn-glycerol-2; DMPE-PEG<sub>2000</sub>, 1,2-dimyristyl-3-trimethylammoniumethyl sulfatate; DSPE-PEG<sub>2000</sub>, 1,2-dimyristyl-3-trimethylammoniumethyl sulfatate; DSPE-PEG<sub>2000</sub>-Mal, 1,2-dimyristyl-3-trimethylammoniumethyl sulfatate-maleimide; DiLA<sup>2</sup>, 1,2-dimyristyl-3-trimethylammoniumethyl sulfatate; C18:1-norarg-C16, 18:1-norargemide; cholesterol, cholesterol; CHEMS, cholesteryl hemisuccinate; DLin, 1,3-bis(sn-3'-phosphatidyl)-sn-glycerol-2; DSPC, 1,3-bis(sn-3'-phosphatidyl)-sn-glycerol-2; PEG-DMG, 1-(monomethoxy poly(ethylene glycol))-2,3-dimyristylglycerol.

Table 6 Summary and characteristics of liposomal formulations for bladder cancer PDT<sup>a</sup>

Composition name	Synthetic components	Functionalization	Size (nm)	Therapeutic agents	Advantages	Administration method
LT <sup>143</sup>	DPPC	Photosensitizer-based liposomes	—	TiO <sub>2</sub>	- Enhanced TiO <sub>2</sub> encapsulation - Increased necrotic and apoptotic effects with UVA exposure - Higher oxidative stress and tumor growth inhibition	Intratumoral injection with irradiation
Tf-Lip-ALPcS <sub>4</sub> (ref. 144)	DSPC, DSPE-PEG <sub>2000</sub> , DSPE-PEG-maleimide, cholesterol	Transferrin-targeting, photosensitizer-based liposomes	146 nm	ALPcS <sub>4</sub>	- Targeted delivery to transferrin receptor-expressing cells - Enhanced tumor selectivity - Increased cellular uptake and photocytotoxicity	Intratumoral injection with irradiation

<sup>a</sup> DPPC, 1,2-dipalmitoyl-*sn*-glycero-3-phosphocholine; DSPC, distearoyl phosphatidylcholine.

respond to particular stimuli, ensuring targeted release at the desired location, and thereby improving the therapeutic efficacy, while reducing adverse effects. Research has explored liposomes that respond to diverse stimuli, including temperature changes, pH fluctuations, enzymatic activity, light, magnetic field, electrical field, and ultrasound.<sup>145</sup> Among them, pH sensitivity demonstrates significant promise due to the presence of multiple pH gradients within the human body.<sup>146</sup>

### 9.1 pH-sensitive liposomes

pH-sensitive liposomes exploit the acidic microenvironment of tissues such as tumors or inflamed areas for targeted drug delivery. These liposomes are stable at physiological pH (7.4) but undergo structural changes in acidic environments (*e.g.*, pH 6.5), enhancing drug release and cellular uptake.

Vila-Caballer *et al.* developed a pH-sensitive liposomal system to efficiently deliver therapeutic proteins to the bladder epithelium. The formulation included methoxy-poly(ethylene glycol)-5 kDa-1,2-distearoyl-*sn*-glycero-3-phosphoethanolamine (mPEG5 kDa-DSPE) and stearoyl-poly(ethylene glycol)-poly(methacryloyl sulfadimethoxine) copolymer (stearoyl-PEG-polySDM). When exposed to acidic urine, the liposomes aggregated, improving their adhesion to the bladder epithelium. *In vitro* studies with mouse BC cells (MB49) and macrophages showed greater liposome uptake at pH 6.5 than at pH 7.4. *In vivo* tests confirmed that the liposomes adhered to the bladder epithelium and delivered the model protein, bovine serum albumin (BSA). Given that it was administered *via* bladder instillation, this system avoided rapid clearance by the reticuloendothelial system, allowing localized delivery. However, its higher polymer density increased the particle size and heterogeneity, suggesting the need for future optimization to balance the therapeutic efficacy, pH sensitivity, and stability.<sup>26</sup>

### 9.2 PEGylated liposomes

Another useful liposome modification involves coating with biocompatible polymers, such as poly(ethylene glycol) (PEG), making liposomes invisible to phagocytes, which are termed “stealth” liposomes. The length and density of the polymer

chains on the liposome surface dictate their circulatory half-life, enabling the development of stable liposomes.<sup>59</sup> This extended circulation enhances passive accumulation in cancerous tissues *via* the enhanced permeation and retention (EPR) effect, ultimately improving the therapeutic efficacy.<sup>147</sup> In addition, PEGylation enhances the surface properties of liposomes through steric hindrance.<sup>148–150</sup> Intravesical drug administration is widely used to deliver therapeutic agents directly to the bladder, but its main limitation is poor drug retention due to urine voiding.

Thus, to address this challenge, a study explored the use of maleimide-functionalized PEGylated liposomes (PEG-Mal) as mucoadhesive carriers for drug delivery to the bladder. The researchers synthesized and characterized three liposomal formulations, conventional liposomes, PEGylated liposomes, and maleimide-functionalized PEGylated liposomes. These formulations were evaluated for their ability to adhere to the bladder mucosa, penetrate the mucosal barrier, and control the release of a model drug, fluorescein sodium. The findings demonstrated that the maleimide-functionalized liposomes exhibited significantly superior retention in the bladder mucosa due to the formation of covalent bonds with the thiol groups in mucin, outperforming both conventional and PEGylated liposomes. Although the PEGylated liposomes exhibited weaker mucoadhesion, they achieved greater mucosal penetration, which is likely due to their stealth properties. Additionally, the maleimide-functionalized liposomes exhibited a slower, sustained drug release profile, thereby extending the therapeutic window. These findings suggest that maleimide-functionalized liposomes show considerable potential for enhancing intravesical drug delivery by improving their retention and offering controlled drug release. These advancements can be particularly beneficial for treating bladder diseases, such as cancer, by optimizing localized drug exposure and minimizing systemic side effects.<sup>151</sup>

Another study focused on addressing the challenges of stability in urine and cellular uptake for BC therapies. Cationic liposomes (Cat-LPs) were modified with PEG lipids at varying molar percentages to enhance their stability in human urine and improve their cellular uptake. The liposome stability in





Table 7 Summary and characteristics of other functionalized liposomes for bladder cancer therapy<sup>a</sup>

Composition name	Synthetic components	Functionalization	Size (nm)	Therapeutic agents	Advantages	Administration method
pH-RL <sup>26</sup>	mPEG5k-DSPE, stearyl-PEG-polysDM, SPC, cholesterol	pH-responsive liposomes	167 ± 1.6 nm	BSA	<ul style="list-style-type: none"><li>- pH-responsive for targeted delivery</li><li>- Enhanced association with bladder epithelium at acidic pH</li><li>- Prolonged retention in bladder</li></ul>	Intravesical administration
PEG-Mal <sup>151</sup>	PC, cholesterol, PEG <sub>2000</sub> -DSPE Mal	Maleimide functionalized PEGylated liposomes	86 ± 1 nm	Fluorescein sodium	<ul style="list-style-type: none"><li>- Strong mucoadhesion</li><li>- Prolonged retention on bladder mucosa</li><li>- Improved stability and slow release</li></ul>	Intravesical administration
PEG-Cat-LP <sup>152</sup>	DOTAP, Chol, POPC, Chol-PEG2k	PEGylated liposomes	98 ± 4 nm	—	<ul style="list-style-type: none"><li>- Prevents aggregation in urine</li><li>- Enhanced cellular uptake</li><li>- Improved stability</li></ul>	Intravesical administration
Bubble liposome <sup>27</sup>	DSPC, DSPE-PEG(2k)-OMe	Sonodynamic liposomes	800–900 nm	Perfluoropropane gas, luciferase gene	<ul style="list-style-type: none"><li>- Ultrasound-mediated siRNA transfer</li><li>- High siRNA transfection efficiency</li></ul>	Subcutaneous injection with ultrasound irradiation
Acoustic liposome <sup>156</sup>	DSPC, DSPE-PEG(2k)-OMe	Sonodynamic liposomes	198.49 ± 29.83 nm	C3F8 gas, luciferase gene	<ul style="list-style-type: none"><li>- Controlled siRNA release</li><li>- Dual-intensity ultrasound for targeted delivery</li><li>- Enhanced localization of gene delivery</li></ul>	Intravesical administration with ultrasound irradiation
LP-gel <sup>157</sup>	SPC, gellan gum	Liposome-in-gel system	124 ± 7 nm	PTX	<ul style="list-style-type: none"><li>- Increased transfection efficiency</li><li>- Ion-triggered gelation for enhanced retention</li></ul>	Intravesical administration
R-FL/P407 (ref. 158)	SPC, cholesterol, DP <sub>2k</sub> F, poloxamer 407	Folate targeted liposome-in-gel system	150–160 nm	Rapamycin	<ul style="list-style-type: none"><li>- Prolonged drug retention</li><li>- High encapsulation efficiency</li><li>- Enhanced folate receptor-mediated endocytosis</li><li>- Prolonged retention in bladder</li><li>- Controlled release of rapamycin</li></ul>	Intravesical administration

<sup>a</sup> PC, phosphatidylcholine; mPEG5k-DSPE, methoxy polyethylene glycol 5000-1,2-distearoyl-*sn*-glycero-3-phosphoethanolamine; stearyl polyethylene glycol poly(sulfadimethoxine methacrylate); DSPC, 1,2-distearoyl *sn*-glycero-3-phosphocholine; DSPE-PEG(2k)-OMe, *N*-(carbonyl-methoxypolyethyleneglycol 2000)-1,2-distearoyl-*sn*-glycero-3-phosphoethanolamine; SPC, soya phosphatidylcholine; DP<sub>2k</sub>F, distearoylphosphatidylethanolamine-polyethylene glycol<sub>2000</sub>-folate.



human urine was evaluated by measuring turbidity, while cellular uptake by BC cells was assessed using flow cytometry following urine incubation. The results demonstrated the addition of 5 mol% PEG2k or 2 mol% PEG5k prevented Cat-LP aggregation in urine, while incorporating 2 mol% cholesteryl-PEG (Chol-PEG) significantly improved the cellular uptake, despite some aggregation.<sup>152</sup>

### 9.3 Sonosensitive liposome

Fujisawa and colleagues developed an ultrasound-mediated bubble liposome (UBL) system to enhance the efficiency of siRNA delivery to BC cells. Bubble liposomes (BLs) are lipid vesicles containing perfluoropropane nanobubbles within their lipid bilayers. Upon ultrasound (US) irradiation, the cavitation induced by the destruction of these nanobubbles temporarily increases the cell membrane permeability, facilitating the efficient transfection of plasmid DNA.<sup>153–155</sup> This innovative approach offers a potential non-invasive treatment modality, particularly for superficial BC, where conventional therapies may be less effective or cause severe side effects. A study demonstrated that UBL successfully delivered siRNA to BC cells both *in vitro* and *in vivo*. *In vitro*, 26% of RT-112Luc cells were transfected with siRNA, resulting in a significant reduction in luciferase activity ( $p = 0.036$ ) under the optimized conditions of  $1 \text{ W cm}^{-2}$  ultrasound intensity, 10 s exposure, and a  $0.2 \text{ mg mL}^{-1}$  concentration of bubble liposomes. *In vivo*, the luciferase activity in mice was significantly suppressed 48 h post-treatment, although the effect diminished by 72 h, suggesting the need for further optimization to improve the stability of siRNA and extend gene silencing.<sup>27</sup>

Horie and colleagues developed an acoustic liposome delivery system for localized gene delivery in the bladder. This system uses a dual-intensity ultrasound (DIUS) technique, where low-intensity ultrasound directs nanobubbles to the target cells, and high-intensity ultrasound induces nanobubble collapse, increasing the cell membrane permeability and facilitating the entry of therapeutic molecules. Data indicate that this system enables the localized delivery of fluorescent molecules and plasmid DNA, with the delivery efficiency positively correlated with the acoustic energy. However, this method has limitations, including limited delivery area and non-specificity to cancer cells, which can potentially be addressed by modifying the nanobubbles for enhanced selective uptake.<sup>156</sup>

### 9.4 LP-gel system

Furthermore, functional liposomes can prolong the local drug retention and enhance therapeutic effects when combined with hydrogels. The ion-triggered liposome-in-gel (LP-gel) system offers improved adhesion and sustained drug release, providing an innovative approach to enhance the effectiveness of intravesical drug delivery.

GuhaSarke *et al.* innovated a system consisting of nano-sized, fluidizing liposomes loaded with paclitaxel (PTX), integrated into a biopolymeric, urine-triggered hydrogel. The liposomes were designed to optimize cellular penetration across the urothelial barrier, while the hydrogel component enhances

adhesion to the mucin layer of the urothelium. The LP-gel system exhibited high encapsulation efficiency and allowed sustained drug release. *In vitro* studies demonstrated its enhanced urothelial adhesion and improved penetration into the bladder wall. Furthermore, *in vivo* studies revealed prolonged drug retention in the bladder for at least 7 days, which was significantly longer than that of the free drug, while maintaining negligible systemic exposure.<sup>157</sup>

Yoon *et al.* developed an intravesical instillation system utilizing Rap-loaded folate-modified liposomes dispersed within a poloxamer 407 (P407)-based thermoreversible hydrogel. The hydrogel systems rapidly formed a gel upon exposure to the bladder temperature, facilitating controlled drug release. Rapamycin-loaded conventional liposomes (R-CL) and rapamycin-loaded folate-modified liposomes (R-FL) were prepared using the film hydration method combined with a pre-loading technique. The liposomes achieved sizes below 160 nm, an entrapment efficiency of approximately 42%, and a drug loading capacity of  $57 \mu\text{g mg}^{-1}$ . R-FL exhibited enhanced cellular uptake and cytotoxicity in folate receptor-expressing BC cells. *In vitro* studies demonstrated that the Rap-loaded liposomes inhibited mTOR signaling and induced autophagy. *In vivo*, the R-FL/P407 system exhibited the highest tumor growth inhibition, underscoring the potential of this targeted delivery approach (Table 7).<sup>158</sup>

## 10. Conclusions and perspectives

Liposomes have been widely recognized by researchers for their ability to improve the stability, solubility, bioavailability, and prolonged circulation time of therapeutic drugs. In addition to enhancing physical and chemical properties, liposomes can also target tumors through the enhanced permeability and retention (EPR) effect and active targeting mechanisms. Specifically, liposome delivery systems increase the precision of drug delivery by modifying proteins on the liposome surface to bind to BC cells or by exploiting the unique characteristics of the tumor microenvironment. Furthermore, a controllable drug release process can be achieved using techniques such as magnetic particles, thermosensitive liposomes, ultrasound mediation, and other methods. Finally, liposomes can encapsulate multiple therapeutic agents simultaneously, enabling them to work synergistically with PDT, radiotherapy and hyperthermia, offering a potential solution to overcome tumor drug resistance. However, despite these advancements, liposome-based therapies still face significant challenges.

There are also several challenges in the course of therapeutic agent administration. In the case of liposomes administered intravenously, they are rapidly removed by the immune system, especially the mononuclear phagocytic system, which reduces their circulation time and limits their accumulation at the tumor. Thus, to address this issue, future research should focus on extending their circulation time and enhancing their targeting surface modifications. Liposomes and other nanomaterials primarily accumulate at tumor sites *via* the enhanced EPR effect. However, in BC, the effectiveness of the EPR mechanism may be limited by the unique tumor

microenvironment, which often exhibits low vascular permeability. Enhancing the EPR effect or utilizing active targeting strategies, such as ligand modification on the liposome surface, can achieve the selective accumulation of therapeutic agents at the tumor site, thus improving the therapeutic efficacy.

Alternatively, intravesical administration offers a way to avoid certain limitations of intravenous delivery. However, the continuous production of urine causes the instilled drug solutions to be frequently diluted or washed out; meanwhile, the biological barrier of the bladder urothelium restricts drug penetration into deeper tissue layers, leading to inefficient treatment and recurrence. Furthermore, frequent severe local irritation may cause some patients to discontinue bladder infusion therapy, negatively impacting the treatment outcomes. Therefore, future liposome delivery systems should aim to overcome biological barriers by enhancing the drug selectivity for BC cells, extending the retention time at the target sites, and improving the permeability across tissue barriers, which are all crucial for optimizing the therapeutic outcomes.

Based on pre-clinical animal experiments, the translation of basic experiments into clinical application may be more complicated for human disease, and thus more relevant humanized models should be considered in research. Additionally, technical challenges must be addressed, including achieving uniform particle size, optimizing drug encapsulation efficiency, and developing cost-effective synthesis processes.

In the future, the advanced development of liposome delivery systems should focus on designing multifunctional nanoparticles that are more tumor specific and can control drug release. New anti-cancer ingredients and emerging gene therapies can utilize liposomes as carriers or functionalize them to achieve new breakthroughs. In addition, the combination of optical and magnetic resonance imaging technologies will further improve the accuracy of tumor diagnosis and treatment. Liposome technology can also be integrated with other therapeutic technologies, such as liposome-hydrogel composite systems, which combine the drug retention capabilities of hydrogels with the biocompatibility of liposomes to achieve more effective tumor suppression. Overall, current research on liposome-based bladder tumor treatment highlights the broad prospects of liposome delivery technology, offering more solutions for the treatment of bladder tumors. Efficient, safe, and controllable treatment plans for tumors with the aid of liposome nanoparticles will continue to attract attention in the coming years.

## Data availability

No primary research results, software or code have been included and no new data were generated or analysed as part of this review.

## Author contributions

Conceptualization, Xinyu Guo and Yan Zhang; writing-original draft preparation, Xinyu Guo and Yan Zhang; writing-review & editing, Quanyong Liu, Mingquan Xu, Jianzhi Pang, and Bin

Yang; supervision, Xiaofeng Yang and Shuo Rong; funding acquisition, Shuo Rong.

## Conflicts of interest

The authors declare that the research was conducted in the absence of any commercial or financial relationships that could be construed as a potential conflict of interest.

## Acknowledgements

The author(s) declare that financial support was received for the research, authorship, and/or publication of this article. This article is supported by the Natural Science Foundation of Shanxi Province (No. 20210302124284).

## References

- 1 K. B. Tran, J. J. Lang, K. Compton, R. Xu, A. R. Acheson, H. J. Henrikson, J. M. Kocarnik, L. Penberthy, A. Aali and Q. Abbas, *Lancet*, 2022, **400**, 563–591.
- 2 E. M. Messing, C. M. Tangen, S. P. Lerner, D. M. Sahasrabudhe, T. M. Koppie, D. P. Wood Jr, P. C. Mack, R. S. Svatek, C. P. Evans, K. S. Hafez, D. J. Culkin, T. C. Brand, L. I. Karsh, J. M. Holzbeierlein, S. S. Wilson, G. Wu, M. Plets, N. J. Vogelzang and I. M. Thompson Jr, *Jama*, 2018, **319**, 1880–1888.
- 3 R. J. Sylvester, W. Oosterlinck, S. Holmang, M. R. Sydes, A. Birtle, S. Gudjonsson, C. De Nunzio, K. Okamura, E. Kaasinen, E. Solsona, B. Ali-El-Dein, C. A. Tatar, B. A. Inman, J. N'Dow, J. R. Oddens and M. Babjuk, *Eur. Urol.*, 2016, **69**, 231–244.
- 4 J. Bellmunt, A. Orsola, J. J. Leow, T. Wiegel, M. De Santis and A. Horwich, *Ann. Oncol.*, 2014, **25**(suppl 3), iii40–iii48.
- 5 R. J. Sylvester, A. P. Van Der Meijden, W. Oosterlinck, J. A. Witjes, C. Bouffloux, L. Denis, D. W. Newling and K. Kurth, *Eur. Urol.*, 2006, **49**, 466–477.
- 6 A. Lopez-Beltran, M. S. Cookson, B. J. Guercio and L. Cheng, *Br. Med. J.*, 2024, **384**, e076743.
- 7 Y. Bayoumi, T. Heikal and H. Darweish, *Cancer Manage. Res.*, 2014, **6**, 459–465.
- 8 J. Tey, Y. Y. Soon, T. Cheo, K. H. Ooi, F. Ho, B. Vellayappan, D. Chia and B. C. Tai, *In Vivo*, 2019, **33**, 2161–2167.
- 9 A. Mari, D. D'Andrea, M. Abufaraj, B. Foerster, S. Kimura and S. F. Shariat, *Transl. Androl. Urol.*, 2017, **6**, 1081–1089.
- 10 F. Massari, M. Santoni, C. Ciccicarese, M. Brunelli, A. Conti, D. Santini, R. Montironi, S. Cascinu and G. Tortora, *Crit. Rev. Oncol. Hematol.*, 2015, **96**, 81–90.
- 11 R. M. Drayton and J. W. Catto, *Expert Rev. Anticancer Ther.*, 2012, **12**, 271–281.
- 12 A. V. Balar, D. Castellano, P. H. O'Donnell, P. Grivas, J. Vuky, T. Powles, E. R. Plimack, N. M. Hahn, R. de Wit, L. Pang, M. J. Savage, R. F. Perini, S. M. Keefe, D. Bajorin and J. Bellmunt, *Lancet Oncol.*, 2017, **18**, 1483–1492.
- 13 A. V. Balar, M. D. Galsky, J. E. Rosenberg, T. Powles, D. P. Petrylak, J. Bellmunt, Y. Loriot, A. Necchi, J. Hoffman-Censits, J. L. Perez-Gracia, N. A. Dawson,



- M. S. van der Heijden, R. Dreicer, S. Srinivas, M. M. Retz, R. W. Joseph, A. Drakaki, U. N. Vaishampayan, S. S. Sridhar, D. I. Quinn, I. Durán, D. R. Shaffer, B. J. Eigl, P. D. Grivas, E. Y. Yu, S. Li, E. E. Kadel III, Z. Boyd, R. Bourgon, P. S. Hegde, S. Mariathasan, A. Thåström, O. O. Abidoye, G. D. Fine and D. F. Bajorin, *Lancet*, 2017, **389**, 67–76.
- 14 M. S. van der Heijden, Y. Lorient, I. Durán, A. Ravaud, M. Retz, N. J. Vogelzang, B. Nelson, J. Wang, X. Shen and T. Powles, *Eur. Urol.*, 2021, **80**, 7–11.
- 15 P. L. Crispin and S. Kusmartsev, *Cancer Immunol., Immunother.*, 2020, **69**, 3–14.
- 16 Y. Zhang, R. Yu, C. Zhao, J. Liang, Y. Zhang, H. Su, J. Zhao, H. Wu, S. Xu, Z. Zhang, L. Wang, X. Zou, Y. Zhu, S. Zhang and Y. Lv, *Adv. Sci.*, 2024, **11**, e2305279.
- 17 J. Chen, C. Fang, C. Chang, K. Wang, H. Jin, T. Xu, J. Hu, W. Wu, E. Shen and K. Zhang, *Colloids Surf., B*, 2024, **234**, 113710.
- 18 K. Wang, S. Zhu, Y. Zhang, Y. Wang, Z. Bian, Y. Lu, Q. Shao, X. Jin, X. Xu and R. Mo, *J. Controlled Release*, 2024, **375**, 589–600.
- 19 D. D. Lasic, F. J. Martin, A. Gabizon, S. K. Huang and D. Papahadjopoulos, *Biochim. Biophys. Acta*, 1991, **1070**, 187–192.
- 20 A. A. Gabizon, *Clin. Cancer Res.*, 2001, **7**, 223–225.
- 21 S. Lv, R. Jing, X. Liu, H. Shi, Y. Shi, X. Wang, X. Zhao, K. Cao and Z. Lv, *Int. J. Nanomed.*, 2021, **16**, 7759–7772.
- 22 M. Ghaferi, M. J. Asadollahzadeh, A. Akbarzadeh, H. Ebrahimi Shahmabadi and S. E. Alavi, *Int. J. Mol. Sci.*, 2020, **21**, 559.
- 23 C. Ma, X. Zhong, R. Liu, X. Yang, Z. Xie, Y. Zhang, Y. Xu, H. Wang, C. He, G. Du, T. Gong and X. Sun, *J. Controlled Release*, 2024, **365**, 640–653.
- 24 F. J. P. van Valenberg, I. S. G. Brummelhuis, L. H. Lindner, F. Kuhnle, B. Wedmann, P. Schweizer, M. Hossann, J. A. Witjes and E. Oosterwijk, *Int. J. Nanomed.*, 2021, **16**, 75–88.
- 25 I. S. G. Brummelhuis, M. Simons, L. H. Lindner, S. Kort, S. de Jong, M. Hossann, J. A. Witjes and E. Oosterwijk, *Int. J. Hyperthermia*, 2021, **38**, 1415–1424.
- 26 M. Vila-Caballer, G. Codolo, F. Munari, A. Malfanti, M. Fassan, M. Rugge, A. Balasso, M. de Bernard and S. Salmaso, *J. Controlled Release*, 2016, **238**, 31–42.
- 27 S. Fujisawa, H. Arakawa, R. Suzuki, K. Maruyama, T. Kodama, M. Yasunaga, Y. Koga and Y. Matsumura, *Ther. Delivery*, 2010, **1**, 247–255.
- 28 C. L. Saw, P. W. Heng and M. Olivo, *J. Environ. Pathol., Toxicol. Oncol.*, 2008, **27**, 23–33.
- 29 J. J. Sonju, A. Dahal, S. S. Singh, X. Gu, W. D. Johnson, C. M. R. Muthumula, S. A. Meyer and S. D. Jois, *Int. J. Pharm.*, 2022, **612**, 121364.
- 30 B. Ji, M. Wei and B. Yang, *Theranostics*, 2022, **12**, 434–458.
- 31 X. Li, W. Li, M. Wang and Z. Liao, *J. Controlled Release*, 2021, **335**, 437–448.
- 32 B. S. Pattni, V. V. Chupin and V. P. Torchilin, *Chem. Rev.*, 2015, **115**, 10938–10966.
- 33 J. C. Kraft, J. P. Freeling, Z. Wang and R. J. Ho, *J. Pharm. Sci.*, 2014, **103**, 29–52.
- 34 S. Shah, V. Dhawan, R. Holm, M. S. Nagarsenker and Y. Perrie, *Adv. Drug Delivery Rev.*, 2020, **154–155**, 102–122.
- 35 R. Tenchov, R. Bird, A. E. Curtze and Q. Zhou, *ACS Nano*, 2021, **15**, 16982–17015.
- 36 C. Pidgeon, S. McNeely, T. Schmidt and J. E. Johnson, *Biochemistry*, 1987, **26**, 17–29.
- 37 R. Koynova and B. Tenchov, *Recent Pat. Nanotechnol.*, 2015, **9**, 86–93.
- 38 D. Carugo, E. Bottaro, J. Owen, E. Stride and C. Nastruzzi, *Sci. Rep.*, 2016, **6**, 25876.
- 39 L. Capretto, D. Carugo, S. Mazzitelli, C. Nastruzzi and X. Zhang, *Adv. Drug Delivery Rev.*, 2013, **65**, 1496–1532.
- 40 S. Joshi, M. T. Hussain, C. B. Roces, G. Anderluzzi, E. Kastner, S. Salmaso, D. J. Kirby and Y. Perrie, *Int. J. Pharm.*, 2016, **514**, 160–168.
- 41 E. Kastner, V. Verma, D. Lowry and Y. Perrie, *Int. J. Pharm.*, 2015, **485**, 122–130.
- 42 E. Kastner, R. Kaur, D. Lowry, B. Moghaddam, A. Wilkinson and Y. Perrie, *Int. J. Pharm.*, 2014, **477**, 361–368.
- 43 H. M. Pang, J. Kenseth and S. Coldiron, *Drug Discovery Today*, 2004, **9**, 1072–1080.
- 44 H. Elsansa, T. O. B. Olusanya, J. Carr-Wilkinson, S. Darby, A. Faheem and A. A. Elkordy, *Sci. Rep.*, 2019, **9**, 15120.
- 45 H. Harashima, K. Sakata, K. Funato and H. Kiwada, *Pharm. Res.*, 1994, **11**, 402–406.
- 46 L. Sercombe, T. Veerati, F. Moheimani, S. Y. Wu, A. K. Sood and S. Hua, *Front. Pharmacol.*, 2015, **6**, 286.
- 47 A. Nagayasu, K. Uchiyama and H. Kiwada, *Adv. Drug Delivery Rev.*, 1999, **40**, 75–87.
- 48 B. William, P. Noémie, E. Brigitte and P. Géraldine, *Chem. Eng. J.*, 2020, **383**, 123106.
- 49 T. M. Allen and J. M. Everest, *J. Pharmacol. Exp. Ther.*, 1983, **226**, 539–544.
- 50 M. Danaei, M. Dehghankhold, S. Ataei, F. Hasanazadeh Davarani, R. Javanmard, A. Dokhani, S. Khorasani and M. R. Mozafari, *Pharmaceutics*, 2018, **10**, 57.
- 51 M. C. Smith, R. M. Crist, J. D. Clogston and S. E. McNeil, *Anal. Bioanal. Chem.*, 2017, **409**, 5779–5787.
- 52 M. Manconi, J. Aparicio, A. O. Vila, J. Pendás, J. Figueruelo and F. Molina, *Colloids Surf., A*, 2003, **222**, 141–145.
- 53 C. Freitas and R. H. Muller, *Int. J. Pharm.*, 1998, **168**, 221–229.
- 54 D. Guimarães, A. Cavaco-Paulo and E. Nogueira, *Int. J. Pharm.*, 2021, **601**, 120571.
- 55 J. L. Betker, D. Jones, C. R. Childs, K. M. Helm, K. Terrell, M. A. Nagel and T. J. Anchordoquy, *J. Controlled Release*, 2018, **286**, 85–93.
- 56 M. K. Riaz, M. A. Riaz, X. Zhang, C. Lin, K. H. Wong, X. Chen, G. Zhang, A. Lu and Z. Yang, *Int. J. Mol. Sci.*, 2018, **19**, 195.
- 57 M. J. Ernsting, M. Murakami, A. Roy and S. D. Li, *J. Controlled Release*, 2013, **172**, 782–794.
- 58 G. Storm, S. O. Belliot, T. Daemen and D. D. Lasic, *Adv. Drug Delivery Rev.*, 1995, **17**, 31–48.



- 59 S. Hassan, G. Prakash, A. Ozturk, S. Saghaazadeh, M. F. Sohail, J. Seo, M. Dockmeci, Y. S. Zhang and A. Khademhosseini, *Nano today*, 2017, **15**, 91–106.
- 60 H. Hatakeyama, H. Akita and H. Harashima, *Biol. Pharm. Bull.*, 2013, **36**, 892–899.
- 61 S. Biswas and V. P. Torchilin, *Adv. Drug Delivery Rev.*, 2014, **66**, 26–41.
- 62 J. Fang, H. Nakamura and H. Maeda, *Adv. Drug Delivery Rev.*, 2011, **63**, 136–151.
- 63 J. C. Kraft, J. P. Freeling, Z. Y. Wang and R. J. Y. Ho, *J. Pharm. Sci.*, 2014, **103**, 29–52.
- 64 P. P. Deshpande, S. Biswas and V. P. Torchilin, *Nanomedicine*, 2013, **8**, 1509–1528.
- 65 J. D. Byrne, T. Betancourt and L. Brannon-Peppas, *Adv. Drug Delivery Rev.*, 2008, **60**, 1615–1626.
- 66 V. P. Torchilin, *Crit. Rev. Ther. Drug Carrier Syst.*, 1985, **2**, 65–115.
- 67 R. J. Lee and P. S. Low, *J. Biol. Chem.*, 1994, **269**, 3198–3204.
- 68 C. P. Leamon and J. A. Reddy, *Adv. Drug Delivery Rev.*, 2004, **56**, 1127–1141.
- 69 X. M. Li, L. Y. Ding, Y. L. Xu, Y. L. Wang and Q. N. Ping, *Int. J. Pharm.*, 2009, **373**, 116–123.
- 70 S. K. Kim and L. Huang, *J. Controlled Release*, 2012, **157**, 279–286.
- 71 J. Zhou, W. Y. Zhao, X. Ma, R. J. Ju, X. Y. Li, N. Li, M. G. Sun, J. F. Shi, C. X. Zhang and W. L. Lu, *Biomaterials*, 2013, **34**, 3626–3638.
- 72 E. Heidarli, S. Dadashzadeh and A. Haeri, *Iran. J. Pharm. Res.*, 2017, **16**, 1273–1304.
- 73 H. Alrbyawi, *Pharmaceutics*, 2024, **16**, 966.
- 74 T. Ta and T. M. Porter, *J. Controlled Release*, 2013, **169**, 112–125.
- 75 C. Das, C. Martín, S. Habermann, H. R. Walker, J. Iqbal, J. Elies, H. S. Jones, G. Reina and A. Ruiz, *Int. J. Mol. Sci.*, 2024, **25**, 115.
- 76 M. A. Rahim, A. Madni, N. Tahir, N. Jan, H. Shah, S. Khan, R. Ullah, A. Bari and M. S. Khan, *Pharmaceutics*, 2021, **13**, 1310.
- 77 H. von der Maase, S. W. Hansen, J. T. Roberts, L. Dogliotti, T. Oliver, M. J. Moore, I. Bodrogi, P. Albers, A. Knuth, C. M. Lippert, P. Kerbrat, P. Sanchez Rovira, P. Wersall, S. P. Cleall, D. F. Roychowdhury, I. Tomlin, C. M. Visseren-Grul and P. F. Conte, *J. Clin. Oncol.*, 2023, **41**, 3881–3890.
- 78 L. Denis, *Lancet*, 1983, **1**, 1378–1379.
- 79 W. Kamoun, E. Swindell, C. Pien, L. Luus, J. Cain, M. Pham, I. Kandela, Z. R. Huang, S. K. Tipparaju, A. Koshkaryev, V. Askoxylakis, D. B. Kirpotin, T. Bloom, M. Mino-Kenudson, J. D. Marks, A. Zalutskaya, W. Bshara, C. Morrison and D. C. Drummond, *Pharmaceutics*, 2020, **12**, 996.
- 80 Z. Chang, M. Gao, W. Zhang, L. Song, Y. Jia and Y. Qin, *Surgical Oncology*, 2017, **26**, 333–337.
- 81 B. Zhai, Q. Wu, W. Wang, M. Zhang, X. Han, Q. Li, P. Chen, X. Chen, X. Huang, G. Li, Q. Zhang, R. Zhang, Y. Xiang, S. Liu, T. Duan, J. Lou, T. Xie and X. Sui, *Cancer Biol. Med.*, 2020, **17**, 60–75.
- 82 B. Zhai, P. Chen, W. Wang, S. Liu, J. Feng, T. Duan, Y. Xiang, R. Zhang, M. Zhang, X. Han, X. Chen, Q. Li, G. Li, Y. Liu, X. Huang, W. Zhang, T. Pan, L. Yan, T. Jin, T. Xie and X. Sui, *Cancer Biol. Med.*, 2020, **17**, 676–692.
- 83 A. Semlali, C. Contant, B. Al-Otaibi, I. Al-Jammaz and F. Chandad, *Sci. Rep.*, 2021, **11**, 11701.
- 84 C. Liu, M. Rokavec, Z. Huang and H. Hermeking, *Cell Death Differ.*, 2023, **30**, 1771–1785.
- 85 S. Gökçe Kütük, G. Gökçe, M. Kütük, H. E. Gürses Cila and M. Nazıroğlu, *Sci. Rep.*, 2019, **9**, 17784.
- 86 L. Gholami, A. A. Momtazi-Borojeni, B. Malaekhe-Nikouei, B. Nikfar, F. Amanolahi, A. Mohammadi and R. Kazemi Oskuee, *Curr. Pharm. Des.*, 2023, **29**, 1046–1058.
- 87 L. Piwowarczyk, M. Kucinska, S. Tomczak, D. T. Mlynarczyk, J. Piskorz, T. Goslinski, M. Murias and A. Jelinska, *Nanomaterials*, 2022, **12**, 1274.
- 88 B. Kneidl, M. Peller, G. Winter, L. H. Lindner and M. Hossann, *Int. J. Nanomed.*, 2014, **9**, 4387–4398.
- 89 A. A. Manzoor, L. H. Lindner, C. D. Landon, J. Y. Park, A. J. Simnick, M. R. Dreher, S. Das, G. Hanna, W. Park, A. Chilkoti, G. A. Koning, T. L. ten Hagen, D. Needham and M. W. Dewhirst, *Cancer Res.*, 2012, **72**, 5566–5575.
- 90 P. Srivastava, *Annu. Rev. Immunol.*, 2002, **20**, 395–425.
- 91 H. I. Robins, M. Kutz, G. J. Wiedemann, D. M. Katschinski, D. Paul, E. Grosen, C. L. Tiggelaar, D. Spriggs, W. Gillis and F. d'Oleire, *Cancer Lett.*, 1995, **97**, 195–201.
- 92 Q. Chen, D. T. Fisher, K. A. Clancy, J. M. Gauguier, W. C. Wang, E. Unger, S. Rose-John, U. H. von Andrian, H. Baumann and S. S. Evans, *Nat. Immunol.*, 2006, **7**, 1299–1308.
- 93 A. S. Mikhail, A. H. Negussie, W. F. Pritchard, D. Haemmerich, D. Woods, I. Bakhutashvili, J. Esparza-Trujillo, S. J. Brancato, J. Karanian, P. K. Agarwal and B. J. Wood, *Int. J. Hyperthermia*, 2017, **33**, 733–740.
- 94 M. Panteliadou, S. Touloupidis, A. Giatromanolaki, K. Pistevo, G. Kyrgias, P. Tsoutsou, C. Kalaitzis and M. I. Koukourakis, *Med. Oncol.*, 2011, **28**, 1356–1362.
- 95 H. W. Herr and A. Morales, *J. Urol.*, 2008, **179**, 53–56.
- 96 T. L. Ratliff, J. O. Palmer, J. A. McGarr and E. J. Brown, *Cancer Res.*, 1987, **47**, 1762–1766.
- 97 H. W. Sinn, B. D. Elzey, R. J. Jensen, X. Zhao, W. Zhao and T. L. Ratliff, *Cancer Immunol., Immunother.*, 2008, **57**, 573–579.
- 98 T. L. Ratliff, L. R. Kavoussi and W. J. Catalona, *J. Urol.*, 1988, **139**, 410–414.
- 99 G. Mora-Bau, A. M. Platt, N. van Rooijen, G. J. Randolph, M. L. Albert and M. A. Ingersoll, *PLoS Pathog.*, 2015, **11**, e1005044.
- 100 M. A. Ingersoll and M. L. Albert, *Mucosal Immunol.*, 2013, **6**, 1041–1053.
- 101 G. Redelman-Sidi, G. Iyer, D. B. Solit and M. S. Glickman, *Cancer Res.*, 2013, **73**, 1156–1167.
- 102 P. Bakhru, N. Sirisaengtaksin, E. Soudani, S. Mukherjee, A. Khan and C. Jagannath, *Cell. Immunol.*, 2014, **287**, 53–61.
- 103 A. M. Kamat, J. Briggman, D. L. Urbauer, R. Svatek, G. M. Nogueras González, R. Anderson, H. B. Grossman, F. Prat and C. P. Dinney, *Eur. Urol.*, 2016, **69**, 197–200.





- 104 J. R. Oddens and T. M. de Reijke, *Eur. Urol.*, 2018, **73**, 749–750.
- 105 W. A. See, G. Zhang, F. Chen, Y. Cao, P. Langenstroer and J. Sandlow, *BJU Int.*, 2009, **103**, 1714–1720.
- 106 C. Ryk, L. R. Koskela, T. Thiel, N. P. Wiklund, G. Steineck, M. C. Schumacher and P. J. de Verdier, *Redox Biol.*, 2015, **6**, 272–277.
- 107 P. F. Severino, M. Silva, M. Carrascal, N. Malagolini, M. Chiricolo, G. Venturi, A. Astolfi, M. CATERA, P. A. Videira and F. Dall'Olio, *Oncotarget*, 2017, **8**, 54506–54517.
- 108 P. F. Severino, M. Silva, M. Carrascal, N. Malagolini, M. Chiricolo, G. Venturi, R. Barbaro Forleo, A. Astolfi, M. CATERA, P. A. Videira and F. Dall'Olio, *BMC Cancer*, 2018, **18**, 198.
- 109 K. Decaestecker and W. Oosterlinck, *Res. Rep. Urol.*, 2015, **7**, 157–163.
- 110 T. Nakamura, M. Fukiage, M. Higuchi, A. Nakaya, I. Yano, J. Miyazaki, H. Nishiyama, H. Akaza, T. Ito, H. Hosokawa, T. Nakayama and H. Harashima, *J. Controlled Release*, 2014, **176**, 44–53.
- 111 J. Miyazaki, H. Nishiyama, I. Yano, A. Nakaya, H. Kohama, K. Kawai, A. Joraku, T. Nakamura, H. Harashima and H. Akaza, *Anticancer Res.*, 2011, **31**, 2065–2071.
- 112 A. Joraku, A. Homhuan, K. Kawai, T. Yamamoto, J. Miyazaki, K. Kogure, I. Yano, H. Harashima and H. Akaza, *BJU Int.*, 2009, **103**, 686–693.
- 113 H. Y. Yoon, H. M. Yang, C. H. Kim, Y. T. Goo, G. Y. Hwang, I. H. Chang, Y. M. Whang and Y. W. Choi, *Pharmaceutics*, 2019, **11**, 652.
- 114 Y. M. Whang, D. H. Yoon, G. Y. Hwang, H. Yoon, S. I. Park, Y. W. Choi and I. H. Chang, *Cancers*, 2020, **12**, 3679.
- 115 R. L. Hunter, M. R. Olsen, C. Jagannath and J. K. Actor, *Ann. Clin. Lab. Sci.*, 2006, **36**, 371–386.
- 116 M. Shiga, J. Miyazaki, K. Tanuma, Y. Nagumo, T. Yoshino, S. Kandori, H. Negoro, T. Kojima, R. Tanaka, N. Okiyama, Y. Fujisawa, M. Watanabe, S. Yamasaki, H. Kiyohara, M. Watanabe, T. A. Sato, H. Tahara, H. Nishiyama and I. Yano, *Cancer Immunol., Immunother.*, 2021, **70**, 2529–2543.
- 117 T. Yoshino, J. Miyazaki, T. Kojima, S. Kandori, M. Shiga, T. Kawahara, T. Kimura, T. Naka, H. Kiyohara, M. Watanabe, S. Yamasaki, H. Akaza, I. Yano and H. Nishiyama, *PLoS One*, 2019, **14**, e0209196.
- 118 S. Samaddar, J. Mazur, J. Sargent and D. H. Thompson, *ACS Appl. Bio Mater.*, 2021, **4**, 3178–3188.
- 119 Q. Ding, W. Tang, X. Li, Y. Ding, X. Chen, W. Cao, X. Wang, W. Mo, Z. Su, Q. Zhang and H. Guo, *J. Controlled Release*, 2023, **363**, 221–234.
- 120 T. L. Ratliff, J. K. Ritchey, J. J. Yuan, G. L. Andriole and W. J. Catalona, *J. Urol.*, 1993, **150**, 1018–1023.
- 121 Y. Horiguchi, W. A. Larchian, R. Kaplinsky, W. R. Fair and W. D. Heston, *Gene Ther.*, 2000, **7**, 844–851.
- 122 M. Horinaga, K. M. Harsch, R. Fukuyama, W. Heston and W. Larchian, *Urology*, 2005, **66**, 461–466.
- 123 Q. Wu, R. Mahendran and K. Esuvaranathan, *Clin. Cancer Res.*, 2003, **9**, 4522–4528.
- 124 J. Fan, Y. Liu, L. Liu, Y. Huang, X. Li and W. Huang, *ACS Synth. Biol.*, 2020, **9**, 343–355.
- 125 H. Song, S. L. Hart and Z. Du, *Int. J. Pharm.*, 2021, **592**, 120033.
- 126 F. A. Barr, H. H. Silljé and E. A. Nigg, *Nat. Rev. Mol. Cell Biol.*, 2004, **5**, 429–440.
- 127 K. Strebhardt, L. Kneisel, C. Linhart, A. Bernd and R. Kaufmann, *Jama*, 2000, **283**, 479–480.
- 128 N. Ahmad, *FASEB J.*, 2004, **18**, 5–7.
- 129 K. Strebhardt and A. Ullrich, *Nat. Rev. Cancer*, 2006, **6**, 321–330.
- 130 M. Nogawa, T. Yuasa, S. Kimura, M. Tanaka, J. Kuroda, K. Sato, A. Yokota, H. Segawa, Y. Toda, S. Kageyama, T. Yoshiki, Y. Okada and T. Maekawa, *J. Clin. Invest.*, 2005, **115**, 978–985.
- 131 U. Krafft, S. Tschirdewahn, J. Hess, N. N. Harke, B. Hadaschik, C. Olah, S. Krege, P. Nyirády, A. Szendrői, M. Szücs, O. Módos, E. Székely, H. Reis and T. Szarvas, *Urol. Oncol.*, 2019, **37**, 810.e7–810.e15.
- 132 D. Martínez-García, N. Manero-Rupérez, R. Quesada, L. Korrodi-Gregório and V. Soto-Cerrato, *Med. Res. Rev.*, 2019, **39**, 887–909.
- 133 S. Seth, Y. Matsui, K. Fosnaugh, Y. Liu, N. Vaish, R. Adami, P. Harvie, R. Johns, G. Severson, T. Brown, A. Takagi, S. Bell, Y. Chen, F. Chen, T. Zhu, R. Fam, I. Maciagiewicz, E. Kwang, M. McCutcheon, K. Farber, P. Charnley, M. E. Houston Jr, A. So, M. V. Templin and B. Polisky, *Mol. Ther.*, 2011, **19**, 928–935.
- 134 M. R. Kang, G. Yang, R. F. Place, K. Charisse, H. Epstein-Barash, M. Manoharan and L. C. Li, *Cancer Res.*, 2012, **72**, 5069–5079.
- 135 I. Diamond, S. G. Granelli, A. F. McDonagh, S. Nielsen, C. B. Wilson and R. Jaenicke, *Lancet*, 1972, **2**, 1175–1177.
- 136 X. Li, J. F. Lovell, J. Yoon and X. Chen, *Nat. Rev. Clin. Oncol.*, 2020, **17**, 657–674.
- 137 P. Jichlinski and H. J. Leisinger, *Urol. Res.*, 2001, **29**, 396–405.
- 138 J. Y. Lee, R. R. Diaz, K. S. Cho, M. S. Lim, J. S. Chung, W. T. Kim, W. S. Ham and Y. D. Choi, *J. Urol.*, 2013, **190**, 1192–1199.
- 139 M. Overchuk, R. A. Weersink, B. C. Wilson and G. Zheng, *ACS Nano*, 2023, **17**, 7979–8003.
- 140 M. Ayers, J. Lunceford, M. Nebozhyn, E. Murphy, A. Loboda, D. R. Kaufman, A. Albright, J. D. Cheng, S. P. Kang, V. Shankaran, S. A. Piha-Paul, J. Yearley, T. Y. Seiwert, A. Ribas and T. K. McClanahan, *J. Clin. Invest.*, 2017, **127**, 2930–2940.
- 141 C. Sun, R. Mezzadra and T. N. Schumacher, *Immunity*, 2018, **48**, 434–452.
- 142 W. Xiong, L. Qi, N. Jiang, Q. Zhao, L. Chen, X. Jiang, Y. Li, Z. Zhou and J. Shen, *ACS Appl. Mater. Interfaces*, 2021, **13**, 8026–8041.
- 143 Y. Chihara, K. Fujimoto, H. Kondo, Y. Moriwaka, T. Sasahira, Y. Hirao and H. Kuniyasu, *Pathobiology*, 2007, **74**, 353–358.



- 144 A. S. Derycke, A. Kamuhabwa, A. Gijssens, T. Roskams, D. De Vos, A. Kasran, J. Huwyler, L. Missiaen and P. A. de Witte, *J. Natl. Cancer Inst.*, 2004, **96**, 1620–1630.
- 145 M. A. Rahim, N. Jan, S. Khan, H. Shah, A. Madni, A. Khan, A. Jabar, S. Khan, A. Elhissi, Z. Hussain, H. C. Aziz, M. Sohail, M. Khan and H. E. Thu, *Cancers*, 2021, **13**, 670.
- 146 M. B. Yatvin, W. Kreutz, B. A. Horwitz and M. Shinitzky, *Science*, 1980, **210**, 1253–1255.
- 147 T. L. Andresen, S. S. Jensen and K. Jørgensen, *Prog. Lipid Res.*, 2005, **44**, 68–97.
- 148 F. F. Davis, *Adv. Drug Delivery Rev.*, 2002, **54**, 457–458.
- 149 A. L. Klibanov, K. Maruyama, V. P. Torchilin and L. Huang, *FEBS Lett.*, 1990, **268**, 235–237.
- 150 G. Blume and G. Cevc, *Biochim. Biophys. Acta*, 1990, **1029**, 91–97.
- 151 D. B. Kaldybekov, P. Tonglairoum, P. Opanasopit and V. V. Khutoryanskiy, *Eur. J. Pharm. Sci.*, 2018, **111**, 83–90.
- 152 T. Nakamura, Y. Noma, Y. Sakurai and H. Harashima, *Biol. Pharm. Bull.*, 2017, **40**, 234–237.
- 153 C. M. Newman and T. Bettinger, *Gene Ther.*, 2007, **14**, 465–475.
- 154 T. Li, K. Tachibana, M. Kuroki and M. Kuroki, *Radiology*, 2003, **229**, 423–428.
- 155 Y. Taniyama, K. Tachibana, K. Hiraoka, T. Namba, K. Yamasaki, N. Hashiya, M. Aoki, T. Ogihara, K. Yasufumi and R. Morishita, *Circulation*, 2002, **105**, 1233–1239.
- 156 S. Horie, Y. Watanabe, R. Chen, S. Mori, Y. Matsumura and T. Kodama, *Ultrasound Med. Biol.*, 2010, **36**, 1867–1875.
- 157 S. GuhaSarkar, P. More and R. Banerjee, *J. Controlled Release*, 2017, **245**, 147–156.
- 158 H. Y. Yoon, I. H. Chang, Y. T. Goo, C. H. Kim, T. H. Kang, S. Y. Kim, S. J. Lee, S. H. Song, Y. M. Whang and Y. W. Choi, *Int. J. Nanomed.*, 2019, **14**, 6249–6268.

